AD-A077 125 WISCONSIN UNIV-MADISON MATHEMATICS RESEARCH CENTER F/G 20/4
A NUMERICAL SIMULATION OF NEWTONIAN AND VISCO-ELASTIC FLOW PAST--ETC(U)
JUL 79 P TOWNSEND DAAG29-75-C-0024
UNCLASSIFIED MRC-TSR-1980 NL

| OF |
AD
A077125

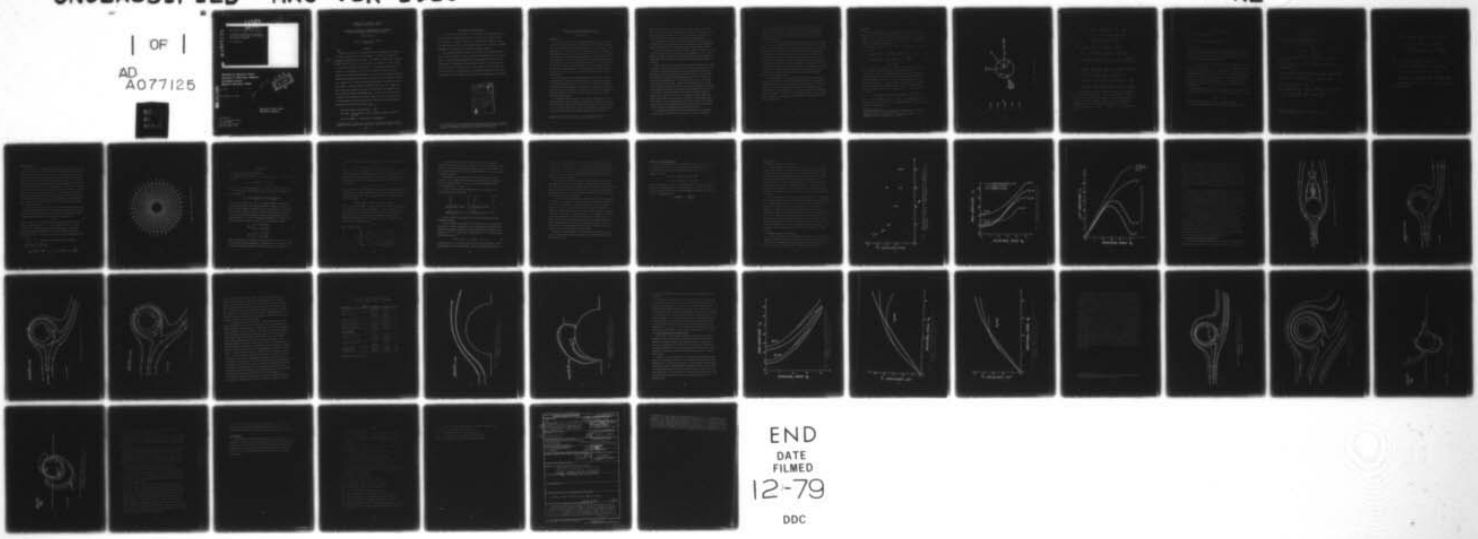

END
DATE
FILMED
12-79
DDC

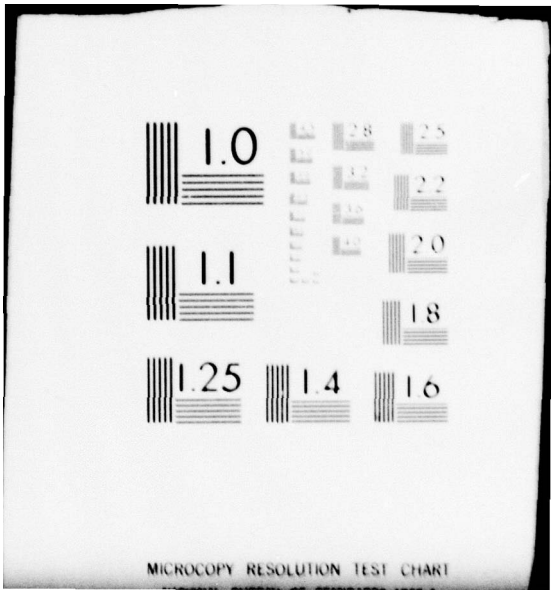
1.0
1.1
1.25
1.4
1.6
2.0
2.2
2.5
MICROCOPY RESOLUTION TEST CHART

MRC Technical Summary Report #1980

A NUMERICAL SIMULATION OF NEWTONIAN AND VISCO-ELASTIC FLOW PAST STATIONARY AND ROTATING CYLINDERS

Peter Townsend

Mathematics Research Center
University of Wisconsin—Madison
610 Walnut Street
Madison, Wisconsin 53706

July 1979

(Received May 31, 1979)

See 1473

Approved for public release
Distribution unlimited

Sponsored by

U.S. Army Research Office
P.O. Box 12211
Research Triangle Park
North Carolina 27709

UNIVERSITY OF WISCONSIN - MADISON
MATHEMATICS RESEARCH CENTER

A NUMERICAL SIMULATION OF NEWTONIAN AND VISCO-ELASTIC FLOW PAST STATIONARY AND ROTATING CYLINDERS

Peter Townsend

Technical Summary Report #1980
July 1979

ABSTRACT

Numerical solutions are presented for the two-dimensional flow past a circular cylinder in an infinite domain. The flow is assumed to be uniform at infinity and the cylinder is allowed to rotate with a constant angular velocity Ω, Ω is chosen to be in the range (0 - 5W/a) where a is the radius of the cylinder and W is the mainstream velocity at infinity. To incorporate visco-elastic properties into the flow, an implicit four constant Oldroyd model is used, and the resulting nonlinear constitutive equations are solved in parallel with the equations of motion as a coupled set of partial differential equations. The method of solution used is a finite difference technique with block over-relaxation. The results are compared with those of other numerical computations as well as with available experimental data. In particular, consideration is given to the influence of cylinder rotation and of visco-elasticity on the drag and lift experienced by the cylinder and on the streamline patterns and vorticity distribution.

AMS (MOS) Subject Classification - 70.65

Key Words - Visco-elastic liquids, Rotating cylinder, Numerical methods

Work Unit Number 3 - Applications of Mathematics

Sponsored by the United States Army under Contract No. DAAG29-75-C-0024.

SIGNIFICANCE AND EXPLANATION

For the past three decades or so rheologists have attempted to derive better and better mathematical models of rheologically complex fluids. The testing of such models, however, for complex flow conditions, has to some extent been neglected. This has been partly due to a lack of adequate mathematical techniques and sufficiently powerful computers.

This report considers one model - the Oldroyd four constant model - which is able to predict elastic and shear-thinning behaviour in a liquid. Numerical solutions are obtained for the two-dimensional flow of such a liquid past a cylinder which rotates about its axis. Such a flow is of interest because the complex nature of the interaction of the main flow and the flow due to the rotation of the cylinder represents a severe test of the ability of the model to represent the true behaviour of the liquid.

The responsibility for the wording and views expressed in this descriptive summary lies with MRC, and not with the author of this report.

A NUMERICAL SIMULATION OF NEWTONIAN AND VISCO-ELASTIC FLOW PAST STATIONARY AND ROTATING CYLINDERS

Peter Townsend

INTRODUCTION

The derivation of more and more sophisticated rheological models of visco-elastic liquids has been the subject of some considerable study over the past three decades or so, and only somewhat lesser attention has been paid to using the models in complex flow situations. The reason for this has to some extent been absence of adequate mathematical techniques, and this is particularly the case for one of the early models - the Oldroyd model. Although some analytical/numerical solutions were obtained for either simple flows or with flow conditions severely restricted in some way by simplifying assumptions, it was not until comparatively recently [1 - 4] that progress was made, and solutions obtained, for more complex flows of an Oldroyd model. Part of this development has been linked to the considerable increase in power of digital computers over the last few years, so that numerical models of sufficient accuracy are now feasible.

The main difference between early semi-analytical/semi-numerical solutions of Oldroyd models and the more recent numerical solutions is that instead of attempting to find approximate expressions for the stress tensor as a function of the velocity distributions, the stress components are considered as dependent variables along with the velocity components and pressure. In other words, in addition to the equations of motion and continuity, one solves the constitutive equations as a set of coupled partial differential equations.

In this paper we apply this technique to a study of two-dimensional flow of an Oldroyd liquid past a circular cylinder, the cylinder rotating about its axis. Such a flow is of interest because of its complexity and also because, even for the special case of a stationary clinder, there is conflicting experimental and theoretical data in the literature as to whether the streamline patterns are moved upstream or

---

Sponsored by the United States Army under Contract No. DAAG29-75-C-0024.

downstream by the presence of elasticity. The interaction of the two basic flows, namely the steady flow and the circulation due to the rotation of the cylinder, results in a strong positional dependence of the rate of strain tensor. The ability of the constitutive equation to represent such a complex flow is severely tested.

It has been found in the past [5] that for some flows in which two separate flow mechanisms interact, although the Oldroyd model is well able to predict qualitatively effects due to shear-thinning, it fails to adequately represent elastic behaviour.

The flow of a Newtonian liquid past a stationary cylinder is certainly not a problem which has been neglected in the literature, see for example [6 - 11]. For this special case we make no attempt to add to existing knowledge, but the availability of several sets of data does provide a useful check on the numerical method employed in this study.

In spite of some very early experiments due to Prandtl and Tietjens [12], in which, in addition to flow visualization studies, they also measured drag and lift forces on the cylinder, there has been comparatively little effort directed to the flow of a Newtonian fluid past a rotating cylinder. Thoman and Szewczyk [13] have calculated time dependent high speed flows, with Reynolds numbers Re of 30, 200 and 10^6, and Phuoc Loc [14] has presented results for very much slower flows ($Re \leq 20$) and slow rotational speeds of the cylinder. Although the two investigations do not overlap, they do draw some contradictory conclusions. In this paper we attempt to resolve some of the contradictions, although since we make the basic assumption of steady flow we do not attempt to consider the higher Reynolds numbers considered by Thoman and Szewczyk, and restrict attention to $Re \leq 40$. Experimental evidence suggests that above a Reynolds number of 40 the flow past a stationary cyclinder becomes unstable and one sees a cyclic time-dependent flow pattern in which vortices are alternately shed downstream from the top and bottom of the cylinder. Where possible, some comparison is made with the experimental data of Prandtl and Tietjens.

If one introduces elasticity into the fluid, then for flow past a stationary cylinder, two basic questions have been considered at length in the literature.

Firstly does elasticity have any effect on the streamline pattern, and if so does it shift the streamlines upstream or downstream relative to the equivalent Newtonian streamlines? Secondly, does the presence of elasticity increase or decrease the Newtonian drag on the cylinder. Some investigations also ask the same questions for shear-thinning behaviour.

From the quite considerable number of investigations carried out, see for example [15 - 23], it seems clear that elasticity decreases the Newtonian drag at low Reynolds numbers and increases the drag at higher Reynolds numbers above unity. On the question of streamline shifting, however, there is complete disagreement. One might expect different fluid models to give different predictions, but even experimental evidence is contradictory. Perhaps some recent work due to Mena [24] may throw some light on the problem in that they claim to be able to show experimentally both upstream and downstream shifting depending on the Weissenberg number. In the present work, because of computational restrictions, we are not able to vary our fluid parameters sufficiently to attempt to predict both upstream and downstream shifting although we are able, to a certain extent, to isolate the separate effects of elasticity and shear-thinning behaviour on the streamline pattern.

To our knowledge there is no existing data, either theoretical or experimental, on visco-elastic flow past a rotating cylinder although it is hoped that some will be available shortly as a result of an experimental investigation by R. B. Bird and R. L. Christiansen, currently in progress at the University of Wisconsin-Madison. As for the stationary case, we again attempt to isolate elastic and shear-thinning behaviour, and present drag and lift coefficients for various Reynolds numbers, rotational speeds and fluid parameters. Streamline projections and vorticity distributions are also given for selected cases.

BASIC THEORY

We consider the steady flow of a visco-elastic liquid past a circular cylinder of radius a and of infinite length. We refer all motion to a set of cylindrical polar coordinates (r,θ,z), where the z axis coincides with the axis of the cylinder (see Figure 1). At some large distance away from the cylinder, the liquid is assumed to flow from left to right with a constant velocity W.

If we take a velocity vector $\underline{v} \equiv (u,v,0)$ then the relevant equations of momentum and continuity are

$$\rho\left[u\frac{\partial u}{\partial r} + \frac{v}{r}\frac{\partial u}{\partial \theta} - \frac{v^2}{r}\right] = -\frac{\partial p}{\partial r} + \frac{\partial p'_{(rr)}}{\partial r} + \frac{1}{r}\frac{\partial p'_{(r\theta)}}{\partial \theta} + \frac{1}{r}\left(p'_{(rr)} - p'_{(\theta\theta)}\right)^{\#} \tag{1}$$

$$\rho\left[u\frac{\partial v}{\partial r} + \frac{v}{r}\frac{\partial v}{\partial \theta} + \frac{uv}{r}\right] = -\frac{1}{r}\frac{\partial p}{\partial \theta} + \frac{\partial p'_{(r\theta)}}{\partial r} + \frac{2}{r}p'_{(r\theta)} + \frac{1}{r}\frac{\partial p'_{(\theta\theta)}}{\partial \theta} \tag{2}$$

$$\frac{\partial u}{\partial r} + \frac{u}{r} + \frac{1}{r}\frac{\partial v}{\partial \theta} = 0 \tag{3}$$

where ρ is the density of the liquid, p denotes the isotropic pressure and $p'_{(rr)}$, $p'_{(r\theta)}$ and $p'_{(\theta\theta)}$ the relevant components of the extra stress tensor.

We need now to select a set of constitutive equations which will characterize our visco-elastic liquid and in doing so we would wish to include both elastic behaviour and a shear dependent viscosity. One of the simpler models available is the four constant Oldroyd model [26]. Although it might be argued that this model is limited to a qualitative picture of viscoelastic behaviour, it has been used successfully in the past for a number of different flow situations (see [25]). The Oldroyd equations are given by

$$p'^{ik} + \lambda_1\frac{\mathcal{D}}{\mathcal{D}t}p'^{ik} + \mu_0 p'^{j}e^{(1)ik} = 2\eta_0\left[e^{(1)ik} + \lambda_2\frac{\mathcal{D}}{\mathcal{D}t}e^{(1)ik}\right]^{\#\#} \tag{4}$$

where η_0 is the zero-shear viscosity, λ_1,λ_2 and μ_0 are time constants, $e^{(1)ik}$ is the rate-of-strain tensor, and $\frac{\mathcal{D}}{\mathcal{D}t}$ is the co-deformational derivative. The relevant components of (4) are given by

---

#Parentheses placed around suffices are used to denote the physical components of tensors. The notation $p_{(ik)}$ corresponds to $-\tau_{ij}$ used in [25].

##Covariant suffices are written below, contravariant suffices above, and the usual summation convention for repeated suffices is implied.

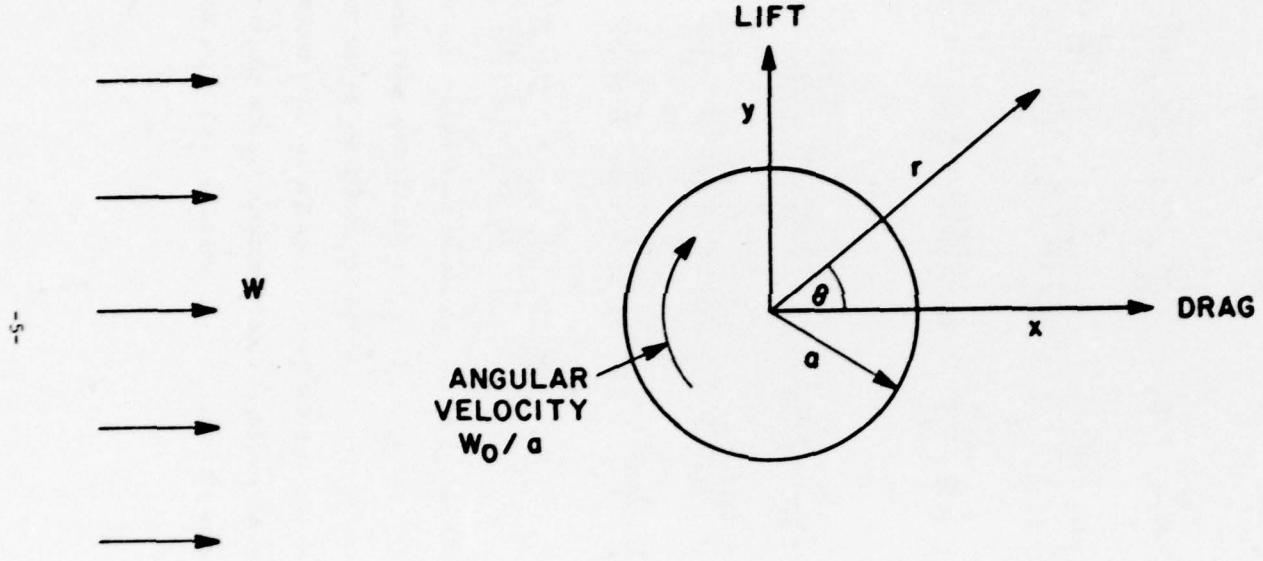

Figure 1. The coordinate system.

$$p'^{rr} + \lambda_1\left[\frac{\partial p'^{rr}}{\partial t} + u\frac{\partial p'^{rr}}{\partial r} + \frac{v}{r}\frac{\partial p'^{rr}}{\partial \theta} - 2\frac{\partial u}{\partial r}p'^{rr} - 2\frac{\partial u}{\partial \theta}p'^{r\theta}\right] \tag{5}$$

$$+ \mu_0\left[p'^{rr} + r^2 p'^{\theta\theta}\right]\frac{\partial u}{\partial r} = 2\eta_0\left[\frac{\partial u}{\partial r} + \lambda_2\left\{\frac{\partial^2 u}{\partial r \partial t} + u\frac{\partial^2 u}{\partial r^2}\right.\right.$$

$$\left.\left. + \frac{v}{r}\frac{\partial^2 u}{\partial r \partial \theta} - 2\left(\frac{\partial u}{\partial r}\right)^2 - \frac{\partial u}{\partial \theta}\left[\frac{\partial}{\partial r}\left(\frac{v}{r}\right) + \frac{1}{r^2}\frac{\partial u}{\partial \theta}\right]\right\}\right],$$

$$p'^{\theta\theta} + \lambda_1\left[\frac{\partial p'^{\theta\theta}}{\partial t} + u\frac{\partial p'^{\theta\theta}}{\partial r} + \frac{v}{r}\frac{\partial p'^{\theta\theta}}{\partial \theta} - 2\frac{\partial\left(\frac{v}{r}\right)}{\partial r}p'^{r\theta} - 2\frac{\partial\left(\frac{v}{r}\right)}{\partial \theta}p'^{\theta\theta}\right] \tag{6}$$

$$+ \mu_0\left[p'^{rr} + r^2 p'^{\theta\theta}\right]\left(\frac{\frac{\partial v}{\partial \theta} + u}{r^3}\right) = 2\eta_0\left[\frac{1}{r^3}\left(\frac{\partial v}{\partial \theta} + u\right) + \lambda_2\left\{\frac{\partial}{\partial t}\left(\frac{\frac{\partial v}{\partial \theta} + u}{r^3}\right)\right.\right.$$

$$\left.\left. + u\frac{\partial}{\partial r}\left(\frac{\frac{\partial v}{\partial \theta} + u}{r^3}\right) + \frac{v}{r}\frac{\partial}{\partial \theta}\left(\frac{\frac{\partial v}{\partial \theta} + u}{r^3}\right) - \frac{\partial}{\partial r}\left(\frac{v}{r}\right)\left[\frac{\partial}{\partial r}\left(\frac{v}{r}\right) + \frac{1}{r^2}\frac{\partial u}{\partial \theta}\right] - 2\frac{\partial\left(\frac{v}{r}\right)}{\partial \theta}\left(\frac{\frac{\partial v}{\partial \theta} + u}{r^3}\right)\right\}\right],$$

and

$$p'^{r\theta} + \lambda_1\left[\frac{\partial p'^{r\theta}}{\partial t} + u\frac{\partial p'^{r\theta}}{\partial r} + \frac{v}{r}\frac{\partial p'^{r\theta}}{\partial \theta} - \frac{\partial u}{\partial r}p'^{r\theta} - \frac{\partial u}{\partial \theta}p'^{\theta\theta} - \frac{\partial\left(\frac{v}{r}\right)}{\partial r}p'^{rr} - \frac{\partial\left(\frac{v}{r}\right)}{\partial \theta}p'^{r\theta}\right] \tag{7}$$

$$+ \frac{\mu_0}{2}\left[p'^{rr} + r^2 p'^{\theta\theta}\right]\left[\frac{\partial}{\partial r}\left(\frac{v}{r}\right) + \frac{1}{r^2}\frac{\partial u}{\partial \theta}\right] = 2\eta_0\left[\frac{1}{2}\left[\frac{\partial}{\partial r}\left(\frac{v}{r}\right) + \frac{1}{r^2}\frac{\partial u}{\partial \theta}\right]\right.$$

$$+ \lambda_2\left\{\frac{1}{2}\frac{\partial}{\partial t}\left[\frac{\partial}{\partial r}\left(\frac{v}{r}\right) + \frac{1}{r^2}\frac{\partial u}{\partial \theta}\right] + \frac{u}{2}\frac{\partial}{\partial r}\left[\frac{\partial}{\partial r}\left(\frac{v}{r}\right) + \frac{1}{r^2}\frac{\partial u}{\partial \theta}\right] + \frac{v}{2r}\frac{\partial}{\partial \theta}\left[\frac{\partial}{\partial r}\left(\frac{v}{r}\right) + \frac{1}{r^2}\frac{\partial u}{\partial \theta}\right]\right.$$

$$\left.\left. - \frac{1}{2}\frac{\partial u}{\partial r}\left[\frac{\partial}{\partial r}\left(\frac{v}{r}\right) + \frac{1}{r^2}\frac{\partial u}{\partial \theta}\right] - \frac{\partial u}{\partial \theta}\left(\frac{\frac{\partial v}{\partial \theta} + u}{r^3}\right) - \frac{\partial\left(\frac{v}{r}\right)}{\partial r}\frac{\partial u}{\partial r} - \frac{1}{2}\frac{\partial\left(\frac{v}{r}\right)}{\partial \theta}\left[\frac{\partial}{\partial r}\left(\frac{v}{r}\right) + \frac{1}{r^2}\frac{\partial u}{\partial \theta}\right]\right\}\right].$$

To complete the specification of the problem we need appropriate boundary conditions on the cylinder and at infinity. Since our stress components are given by a set of differential equations, then in addition to conditions on the velocity components, we require stress boundary conditions. For the infinity boundary it is computationally convenient to specify a steady streaming in the positive 'x' direction on some very large cylinder $r = r_\infty$, where $r_\infty >> a$. The conditions then become

$$u = W\,\mathrm{Cos}\theta, \quad v = -W\,\mathrm{Sin}\theta \tag{8}$$

$$p'_{(rr)} = p'_{(r\theta)} = p'_{(\theta\theta)} = 0$$

On the cylinder we have that

$$u = 0 \tag{9}$$

and if the cylinder rotates with angular velocity Ω, then

$$v = W_0 \tag{10}$$

where $W_0 = a\Omega$.

For the stress components we have no simple expressions that we may write down, and we must look instead at what form the constitutive equations take on the cylinder surface. For brevity we restrict attention for illustration purposes to the '$r\theta$' component equation which may be written in the form

$$p'^{r\theta} + \lambda_1\left[\frac{v}{r}\frac{\partial p'^{r\theta}}{\partial \theta} - \frac{\partial u}{\partial r}p'^{r\theta} - \frac{\partial\left(\frac{v}{r}\right)}{\partial r}p'^{rr}\right] + \frac{\mu_0}{2}\left[p'^{rr} + r^2 p'^{\theta\theta}\right]\frac{\partial}{\partial r}\left(\frac{v}{r}\right) = f(u,v) \tag{11}$$

where f is a known function of u and v. It will be noted that the only stress component derivative which appears in this equation is a 'θ' derivative, so that provided the velocity distribution is known in the fluid, then (11), together with the equivalent 'rr' and '$\theta\theta$' components, represent a set of coupled ordinary differential equations, with cyclic boundary conditions, to be solved for the stress distribution on the cylinder. This forms the basis for an iterative scheme to be described later.

Before attempting to solve the system of equations (1), (2), (5), (6) and (7) we perform a number of simplifications. We first introduce a stream function ψ defined by

$$u = \frac{1}{r}\frac{\partial \psi}{\partial \theta}, \quad v = -\frac{\partial \psi}{\partial r}. \tag{12}$$

With this choice the equation of continuity is satisfied identically.

Secondly we make a transformation into non-dimensional variables as follows

$$r^* = r/a, \quad u^* = u/W, \quad v^* = v/W \tag{13}$$

$$p^* = p/\rho W^2, \quad p^*_{(ik)} = p_{(ik)} \cdot a/\eta_0 W, \quad \psi^* = \psi/aW$$

$$\lambda_1^* = \lambda_1 W/a, \quad \lambda_2^* = \lambda_2 W/a, \quad \mu_0^* = \mu_0 W/a$$

We choose to drop the * notation immediately although it is still implied.

We next make a change of variable as follows

$$p'_{(rr)} = \bar{p}_{(rr)} + 2\frac{\partial u}{\partial r} \tag{14}$$

$$p'_{(\theta\theta)} = \bar{p}_{(\theta\theta)} + 2\left(\frac{1}{r}\frac{\partial v}{\partial \theta} + \frac{u}{r}\right)$$

$$p'_{(r\theta)} = \bar{p}_{(r\theta)} + r\frac{\partial}{\partial r}\left(\frac{v}{r}\right) + \frac{1}{r}\frac{\partial u}{\partial \theta}$$

so that our new 'stress' variables $\bar{p}_{(ik)}$ now represent a deviation from Newtonian flow behaviour.

Finally we eliminate the pressure from the two momentum equations to give

$$\frac{1}{r}\left[\frac{\partial \psi}{\partial \theta}\frac{\partial \omega}{\partial r} - \frac{\partial \psi}{\partial r}\frac{\partial \omega}{\partial \theta}\right] - \frac{1}{R_e}\nabla^2\omega \tag{15}$$

$$= \frac{1}{R_e}\left[\frac{1}{r}\frac{\partial}{\partial \theta}\left\{\frac{\partial \bar{p}_{(rr)}}{\partial r} + \frac{1}{r}\frac{\partial \bar{p}_{(r\theta)}}{\partial \theta} + \frac{(\bar{p}_{(rr)} - \bar{p}_{(\theta\theta)})}{r}\right\} - \frac{1}{r}\frac{\partial}{\partial r}\left\{r\left[\frac{\partial \bar{p}_{(r\theta)}}{\partial r} + 2\frac{\bar{p}_{(r\theta)}}{r} + \frac{1}{r}\frac{\partial \bar{p}_{(\theta\theta)}}{\partial \theta}\right]\right\}\right]$$

where $R_e (=\rho aW/\eta_0)$ is a Reynolds number and ω is the vorticity given by

$$\omega = \nabla^2\psi \ ^{\#} \tag{16}$$

The modified constitutive equations become

$$\bar{p}_{(rr)} + \lambda_1\left[u\frac{\partial \bar{p}_{(rr)}}{\partial r} + \frac{v}{r}\frac{\partial}{\partial \theta}\bar{p}_{(rr)} - 2\frac{\partial u}{\partial r}\bar{p}_{(rr)} - 2\frac{\partial u}{\partial \theta}\frac{\bar{p}_{(r\theta)}}{r}\right] + \mu_0\left[\bar{p}_{(rr)} + \bar{p}_{(\theta\theta)}\right]\frac{\partial u}{\partial r} \tag{17}$$

$$= 2(\lambda_2 - \lambda_1)\left[u\frac{\partial^2 u}{\partial r^2} + \frac{v}{r}\frac{\partial^2 u}{\partial r \partial \theta} - 2\left(\frac{\partial u}{\partial r}\right)^2 - \frac{\partial u}{\partial \theta}\left[\frac{\partial}{\partial r}\left(\frac{v}{r}\right) + \frac{1}{r^2}\frac{\partial u}{\partial \theta}\right]\right],$$

$^{\#}$For this two dimensional problem ω is the magnitude of $\underline{\omega} = [\nabla \wedge \underline{v}]$.

$$\frac{\bar{P}_{(\theta\theta)}}{r^2} + \lambda_1\left[u\frac{\partial}{\partial r}\left(\frac{\bar{P}_{(\theta\theta)}}{r^2}\right) + \frac{v}{r}\frac{\partial}{\partial\theta}\left(\frac{\bar{P}_{(\theta\theta)}}{r^2}\right) - 2\frac{\partial\left(\frac{v}{r}\right)}{\partial r}\frac{\bar{P}_{(r\theta)}}{r} - 2\frac{\partial\left(\frac{v}{r}\right)}{\partial\theta}\frac{\bar{P}_{(\theta\theta)}}{r^2}\right] \tag{18}$$

$$+ \mu_0\left[\bar{P}_{(rr)} + \bar{P}_{(\theta\theta)}\right]\left(\frac{\frac{\partial v}{\partial\theta} + u}{r^3}\right) = 2(\lambda_2 - \lambda_1)\left[u\frac{\partial}{\partial r}\left(\frac{\frac{\partial v}{\partial\theta} + u}{r^3}\right)\right.$$

$$\left. + \frac{v}{r}\frac{\partial}{\partial\theta}\left(\frac{\frac{\partial v}{\partial\theta} + u}{r^3}\right) - \frac{\partial}{\partial r}\left(\frac{v}{r}\right)\left(\frac{\partial}{\partial r}\left(\frac{v}{r}\right) + \frac{1}{r^2}\frac{\partial u}{\partial\theta}\right) - 2\frac{\partial\left(\frac{v}{r}\right)}{\partial\theta}\left(\frac{\frac{\partial v}{\partial\theta} + u}{r^3}\right)\right],$$

and

$$\frac{\bar{P}_{(r\theta)}}{r} + \lambda_1 u\left[\frac{\partial}{\partial r}\left(\frac{\bar{P}_{(r\theta)}}{r}\right) + \frac{v}{r}\frac{\partial}{\partial\theta}\left(\frac{\bar{P}_{(r\theta)}}{r}\right) - \frac{\partial u}{\partial r}\left(\frac{\bar{P}_{(r\theta)}}{r}\right) - \frac{\partial u}{\partial\theta}\left(\frac{\bar{P}_{(\theta\theta)}}{r^2}\right)\right. \tag{19}$$

$$\left. - \frac{\partial}{\partial r}\left(\frac{v}{r}\right)\bar{P}_{(rr)} - \frac{\partial}{\partial\theta}\left(\frac{v}{r}\right)\frac{\bar{P}_{(r\theta)}}{r}\right] + \frac{\mu_0}{2}\left[\bar{P}_{(rr)} + \bar{P}_{(\theta\theta)}\right]\left[\frac{\partial}{\partial r}\left(\frac{v}{r}\right) + \frac{1}{r^2}\frac{\partial u}{\partial\theta}\right]$$

$$= (\lambda_2 - \lambda_1)\left[u\frac{\partial}{\partial r}\left(\frac{\partial}{\partial r}\left(\frac{v}{r}\right) + \frac{1}{r^2}\frac{\partial u}{\partial\theta}\right) + \frac{v}{r}\frac{\partial}{\partial\theta}\left(\frac{\partial}{\partial r}\left(\frac{v}{r}\right) + \frac{1}{r^2}\frac{\partial u}{\partial\theta}\right)\right.$$

$$\left. - \frac{\partial u}{\partial r}\left(\frac{\partial}{\partial r}\left(\frac{v}{r}\right) + \frac{1}{r^2}\frac{\partial u}{\partial\theta}\right) - 2\frac{\partial u}{\partial\theta}\left(\frac{\frac{\partial v}{\partial\theta} + u}{r^3}\right) - 2\frac{\partial\left(\frac{v}{r}\right)}{\partial r}\frac{\partial u}{\partial r} - \frac{\partial\left(\frac{v}{r}\right)}{\partial\theta}\left(\frac{\partial}{\partial r}\left(\frac{v}{r}\right) + \frac{1}{r^2}\frac{\partial u}{\partial\theta}\right)\right]$$

For the Newtonian case we need solve only (15) and (16) with the stress variables set to be identically zero.

NUMERICAL SOLUTION

When one refers to the Oldroyd model as a 'simple' model then one is talking about the 'simple' representation of fluid properties. The coupled nonlinear partial differential equations which one obtains for stress and velocity components from using this model are certainly far from simple to solve, and unless some very restrictive perturbation analysis is employed, one must resort to numerical techniques. In an earlier paper [1], a numerical finite difference solution was presented for pulsatile flow of an Oldroyd fluid in a circular pipe. In this work the coupled stress/velocity equations were solved as an initial value problem, starting from rest, and advanced in time until a steady, or quasi-steady state was obtained. In the present paper, the problem is treated as a boundary value problem in which we seek coupled velocity and stress variables consistent with conditions specified on closed boundaries. This technique has been used by Walters and his co-workers [2-4] for flow through constricted channels and flow around sharp corners.

In order to discretize our equations we need to adopt some finite difference grid. A cylindrical polar grid does not give a very satisfactory distribution of grid points. We need to concentrate grid points near to the cylinder where variables are changing more rapidly, and where greater accuracy is required. Accordingly we set

$$\xi = \log r \tag{20}$$

and work in terms of (ξ,θ) coordinates on the logarithmic grid shown in Figure 2. Twenty grid points were used in the ξ direction and forty in the θ direction. Although this is a somewhat coarser grid than perhaps desirable, one is severely limited by the very considerable amounts of computer arithmetic needed to solve problems of this kind. ξ_∞ was taken to be 3.0 giving an outer non-dimensional radius r^*_∞ of 20.1.

In terms of (ξ,θ) coordinates our modified momentum equations become

$$\left[\frac{\partial\psi}{\partial\theta}\frac{\partial\omega}{\partial\xi} - \frac{\partial\psi}{\partial\xi}\frac{\partial\omega}{\partial\theta}\right] - \frac{1}{R_e}\left[\frac{\partial^2\omega}{\partial\xi^2} + \frac{\partial^2\omega}{\partial\theta^2}\right] \tag{21}$$

$$= \frac{1}{R_e}\left[\frac{\partial}{\partial\theta}\left\{\frac{\partial\bar{P}_{(rr)}}{\partial\xi} + \frac{\partial\bar{P}_{(r\theta)}}{\partial\theta} + \bar{P}_{(rr)} - \bar{P}_{(\theta\theta)}\right\} - \frac{\partial}{\partial\xi}\left\{\frac{\partial\bar{P}_{rr}}{\partial\xi} + 2\bar{P}_{r\theta} + \frac{\partial\bar{P}_{\theta\theta}}{\partial\theta}\right\}\right]$$

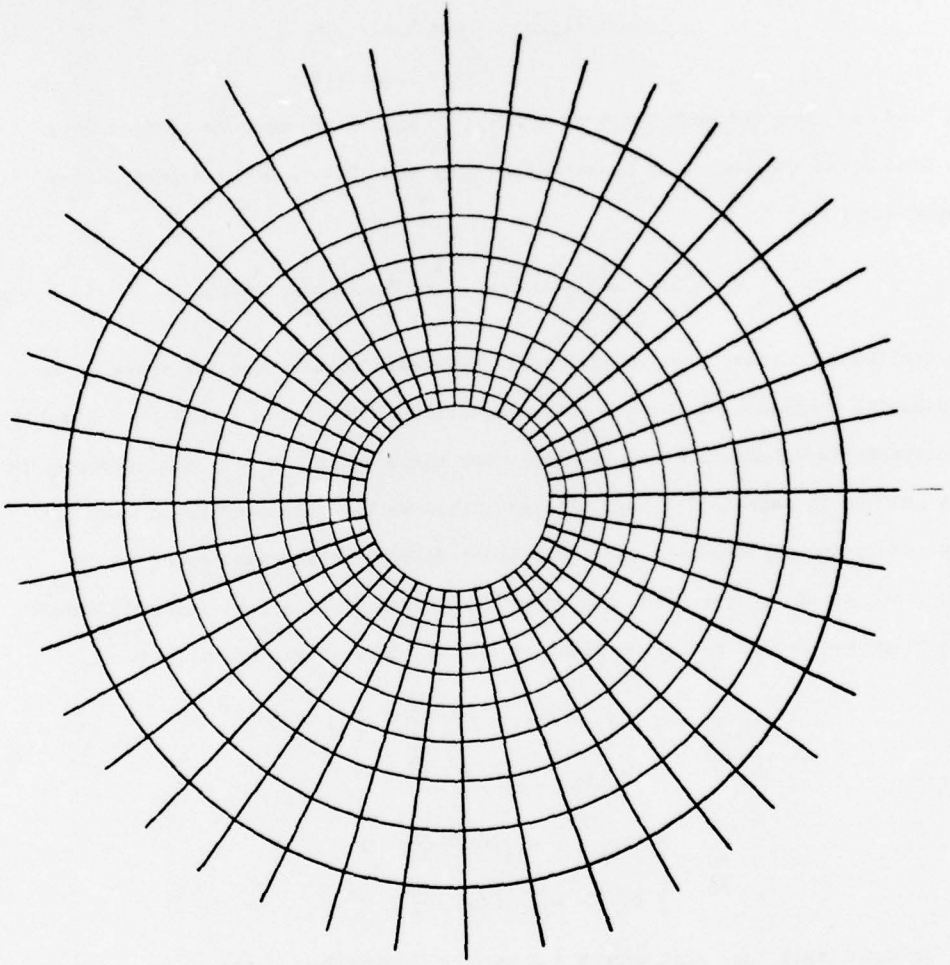

Figure 2. Part of the finite difference grid.

and

$$\frac{\partial^2 \psi}{\partial \xi^2} + \frac{\partial^2 \psi}{\partial \theta^2} = \omega e^{2\xi} \tag{22}$$

and similarly for the constitutive equations.

We introduce discrete variables ψ_{ij}, ω_{ij}, $\bar{P}_{(rr)_{ij}}$, $\bar{P}_{(r\theta)_{ij}}$, and $\bar{P}_{(\theta\theta)_{ij}}$, where for example

$$\psi_{ij} = \psi(i\Delta\xi, j\Delta\theta) \qquad \begin{matrix} i = 1,2,\ldots,M \\ j = 1,2,\ldots,N \end{matrix} \tag{23}$$

and $\Delta\xi$ and $\Delta\theta$ are the mesh spacings in the ξ and θ directions respectively.

To discretize the Laplacian operators in (21) and (22) we use a standard five point approximation

$$\nabla^2 A_{ij} = \frac{A_{i+1j} - 2A_{ij} + A_{i-1j}}{(\Delta\xi)^2} + \frac{A_{ij+1} - 2A_{ij} + A_{ij-1}}{(\Delta\theta)^2} \tag{24}$$

For the nonlinear inertia terms in (21) it is necessary to take special measures to ensure diagonal dominance of the difference equations. Otherwise it has been found that the iterative scheme to be applied to solve these equations will not converge for Reynolds numbers in excess of unity. The technique we have employed is to make use of so-called upwind differencing where one-sided difference approximations to the first derivatives of ω are used, the particular approximation i.e. forward or backward, being chosen according to the signs of the ψ derivatives as follows.

$$\frac{\partial \omega}{\partial \xi} = \begin{cases} (\omega_{ij} - \omega_{i-1j})/\Delta\xi & \frac{\partial \psi}{\partial \theta} > 0 \\ (\omega_{i+1j} - \omega_{ij})/\Delta\xi & \frac{\partial \psi}{\partial \theta} < 0 \end{cases}$$

$$\frac{\partial \omega}{\partial \theta} = \begin{cases} (\omega_{ij+1} - \omega_{ij})/\Delta\theta & \frac{\partial \psi}{\partial \xi} > 0 \\ (\omega_{ij} - \omega_{ij-1})/\Delta\theta & \frac{\partial \psi}{\partial \xi} < 0 \end{cases} \tag{25}$$

Clearly, in doing this, one must accept a loss of accuracy due to the first order nature of the one-sided difference approximations. Greater accuracy can be recovered, however, if required, by applying a difference correction procedure (see, for example, [27]).

With these difference approximations the vorticity equation may be written in the form

$$E_1\omega_{i-1j} + E_2\omega_{i+1j} + E_3\omega_{ij-1} + E_4\omega_{ij+1} + E_5\omega_{ij} = R_{ij} \tag{26}$$

where the E's and R_{ij} are functions of ψ, $\bar{p}_{(rr)}$, $\bar{p}_{(r\theta)}$ and $\bar{p}_{(\theta\theta)}$. One obvious solution technique which can now be applied to solve (26) is to use successive over-relaxation by points at each node of the finite difference grid. In making a sweep through the grid the computer program must incorporate the cyclic boundary condition by recognizing that

$$\omega_{i1} \equiv \omega_{iN}, \quad i = 1,2,\ldots,M \tag{27}$$

Attempts to apply such a scheme proved successful, but the solution was extremely slow to settle down to the symmetric form about the x-axis which one expects in the case of a stationary cylinder. A more satisfactory method which was finally adopted was to write (26) in the form

$$E_1\omega_{i-1j}^{(k)} + E_5\omega_{ij}^{(k)} + E_2\omega_{i+1j}^{(k)} = R_{ij} - E_3\omega_{ij-1}^{(k)} - E_4\omega_{ij+1}^{(k-1)} \tag{28}$$

where k is an iteration number. We may then iterate in blocks, each block consisting of a complete set of ω values for a particular 'i' value. In other words one solves in a series of circles concentric with the cylinder. The tri-diagonal system represented by (2.8) is solved directly using a modified Gaussion elimination algorithm which incorporates the cyclic boundary condition. Essentially one solves a system of linear equations of the form

$$A\underset{\sim}{\omega} = \underset{\sim}{b} \tag{29}$$

where A takes the form

$$A \equiv \begin{bmatrix} a_{11} & a_{12} & 0 \cdots\cdots\cdots\cdots 0 & a_{1,M-1} \\ a_{21} & a_{22} & a_{23} \quad 0 \cdots\cdots\cdots\cdots 0 & \\ 0 & \ddots & \ddots & \ddots \\ \vdots & & & a_{M-2,M-1} \\ 0 & & & \\ a_{M-1,1} & 0 \cdots\cdots\cdots\cdots 0 & a_{M-1,M-2} & a_{M-1,M-1} \end{bmatrix} \tag{30}$$

The discrete forms of the remaining stream function, and stress component equations, and also the boundary stress equations (c.f. (11)), take essentially the same form as (28) and the same block solution algorithm is used in each case. Again, one-sided differences are used to ensure diagonal dominance for some of the nonlinear terms in the stress equations.

The direction of the block iteration used, varies according to the boundary conditions. For the stream function we iterate inwards from the non-zero conditions on the r_∞ boundary, while for ω and $\bar{p}_{(ik)}$ we iterate outwards away from the non-zero conditions on the cylinder.

In order to obtain consistent approximations for all the variables an outer iterative scheme is set up as follows

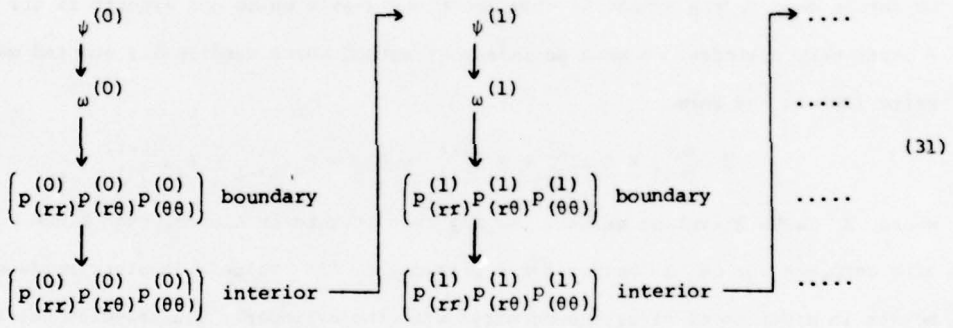

(31)

The outer iteration is continued until two successive iterates agree to some predetermined tolerance.

In order to optimize the convergence of the scheme set out in (31), and indeed, for most cases, to obtain convergence at all, some considerable attention must be paid to smoothing both interior and boundary values of variables. When, for example, a new approximation $\psi^{(n+1)}$ is computed, then a weighted mean $\bar{\psi}^{(n+1)}$ of this value and the previous iterate given by

$$\bar{\psi}^{(n+1)} = \rho_s \psi^{(n)} + (1 - \rho_s)\psi^{(n+1)} \qquad 0 \leq \rho \leq 1 \tag{32}$$

is actually used for ψ for the next stage of the outer iteration procedure. For low Reynolds numbers and low rotational speeds, little or no smoothing was necessary, but

as parameter values increased initial violent oscillations or unbounded growth in the solution had to be dumped out. For ψ,ω and the interior values of the stresses a constant value of 0.95 was used for ρ_s, while for boundary stress and vorticity values, which proved to be more critical, a variable smoothing was applied. Initially a ρ_s value of as high as 0.999 was necessary for some Reynolds numbers, and this was then relaxed as the iteration proceeded.

The block iterative scheme, in addition to faster convergence, has apparently other advantages. Phuoc Loc [14], who used point iteration on a similar grid to that employed here to solve the rotating cylinder problem for a Newtonian liquid, experienced numerical stability problems as the rotational speed is increased. No such problems were apparent for the block iterative scheme and we were able to extend the Phuoc Loc data to a much higher range of parameters.

For the visco-elastic liquid, however, convergence proved to be far more difficult to achieve. If one is prepared to juggle with smoothing parameters then it may well be that a solution is possible for any physically reasonable set of fluid parameters. However, in our experience, the solution of the full visco-elastic problem is very expensive on computer time and with a finite computer budget there seems to be a limit to the degree of nonlinearity in the equations that one can accommodate. This limitation has been experienced by a number of other workers in this field (see [4]). It may well be that the type of iterative scheme outlined in this paper is unsuited for highly nonlinear problems, and that one must turn to other techniques. The use of higher order collocation approximations together with more sophisticated nonlinear equation solvers [28] may well prove to be one possibility.

The majority of the computation of the data presented in this paper was carried out on two DEC VAX computers with run times varying from several minutes to several hours in extreme cases.

COMPUTATION OF ADDITIONAL PARAMETERS

When a fluid flows past the rotating cylinder, the cylinder is subject to a net force in each of the 'x' and 'y' directions, namely the total drag and total lift. To compute these we resolve the pressure and extra stress forces into x and y components as follows

$$F_x = -p\,\mathrm{Cos}\theta + \frac{1}{Re}\left[p'_{(rr)}\mathrm{Cos}\theta - p'_{(r\theta)}\mathrm{Sin}\theta\right] \tag{33}$$

$$F_y = -p\,\mathrm{Sin}\theta + \frac{1}{Re}\left[p'_{(rr)}\mathrm{Sin}\theta + p'_{(r\theta)}\mathrm{Cos}\theta\right] \tag{34}$$

The stress components $p'_{(rr)}$ and $p'_{(r\theta)}$ are obtained from (14) and the pressure distribution found by integrating the 'θ' momentum equation (2). If we then integrate (33) and (34) around the cylinder surface we obtain non-dimensional drag and lift coefficients C_D and C_L respectively, where

$$C_D = \frac{\text{total drag}}{\rho W^2 a}, \quad C_L = \frac{\text{total lift}}{\rho W^2 a} \tag{35}$$

NUMERICAL RESULTS

(i) Newtonian flow past a stationary cylinder

This problem has been covered very extensively in the literature and we do not attempt to add to what has already been said. The extensive numerical data available do however offer one very useful accuracy check on the work presented in this paper, particularly in view of the somewhat coarse finite difference grid used. In Figure 3 we have plotted the drag coefficient as a function of Reynolds number. We have restricted attention to a range of Reynolds numbers where one would expect from experimental evidence to find a stable flow, symmetric about the 'x' axis. For higher Reynolds numbers an instability occurs in which vortices are periodically shed downstream from alternate sides of the cylinder, and in this case a time dependent analysis is necessary.

From the data given in Figure 3 we see that the present work is in good agreement with most previous workers and we feel some confidence therefore in our numerical method. It is noticeable, however, that one set of results due to Thoman and Szewczyk [10] is very much out of line with the bulk of available data and it is not clear why this should be. The Thoman and Szewczyk work does differ, to some extent, from the other investigations in that they do concentrate their work on very high Reynolds number flows up to $Re = 10^6$ and to obtain numerical stability find it necessary to employ a hybrid cartesian/polar grid system. What numerical effects this has are not clear. We only point out these differences between their stationary cylinder work and that of several later investigations because of a number of differences between their rotating cylinder work and the current investigation. These differences will be apparent in the next section.

(ii) Newtonian flow past a rotating cylinder

In spite of some very early flow visualization experiments for this problem [12], theoretical solutions, unlike for the stationary case, have been few in number. The only two sets of numerical data of which we are aware at this time are given, together with the present work, in Figures (4) and (5) where we plot the drag and lift

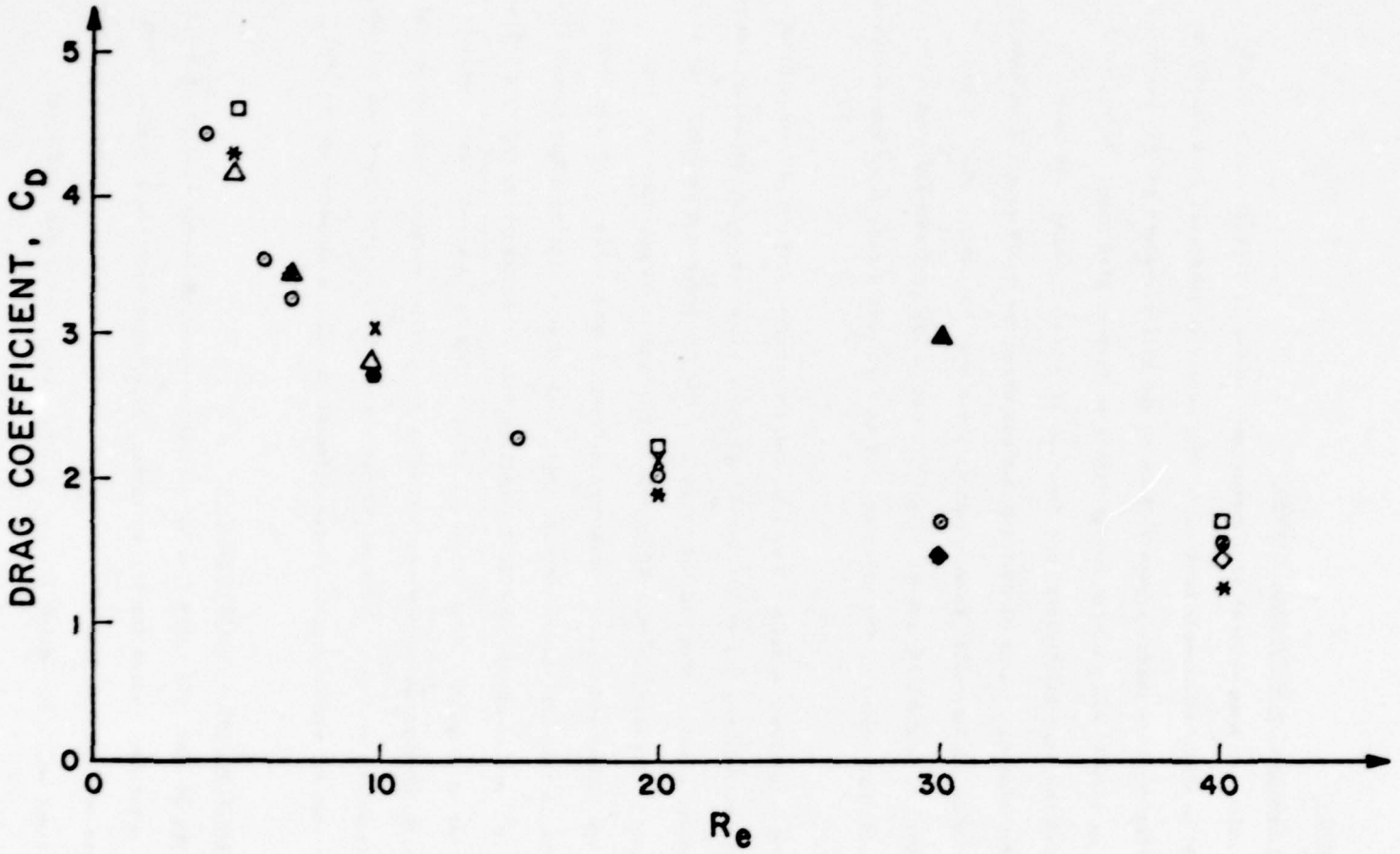

Figure 3. Newtonian drag coefficient C_D (= total drag/$\rho W^2 a$) versus Reynolds number Re for various different investigations. Δ Dennis and Chang [9], θ Takami and Keller [11], □ Phuoc Loc [14], ◊ Apelt [6], ▲ Thoman and Szewczyk [10], X Pilate and Crochet [21], * Present Study

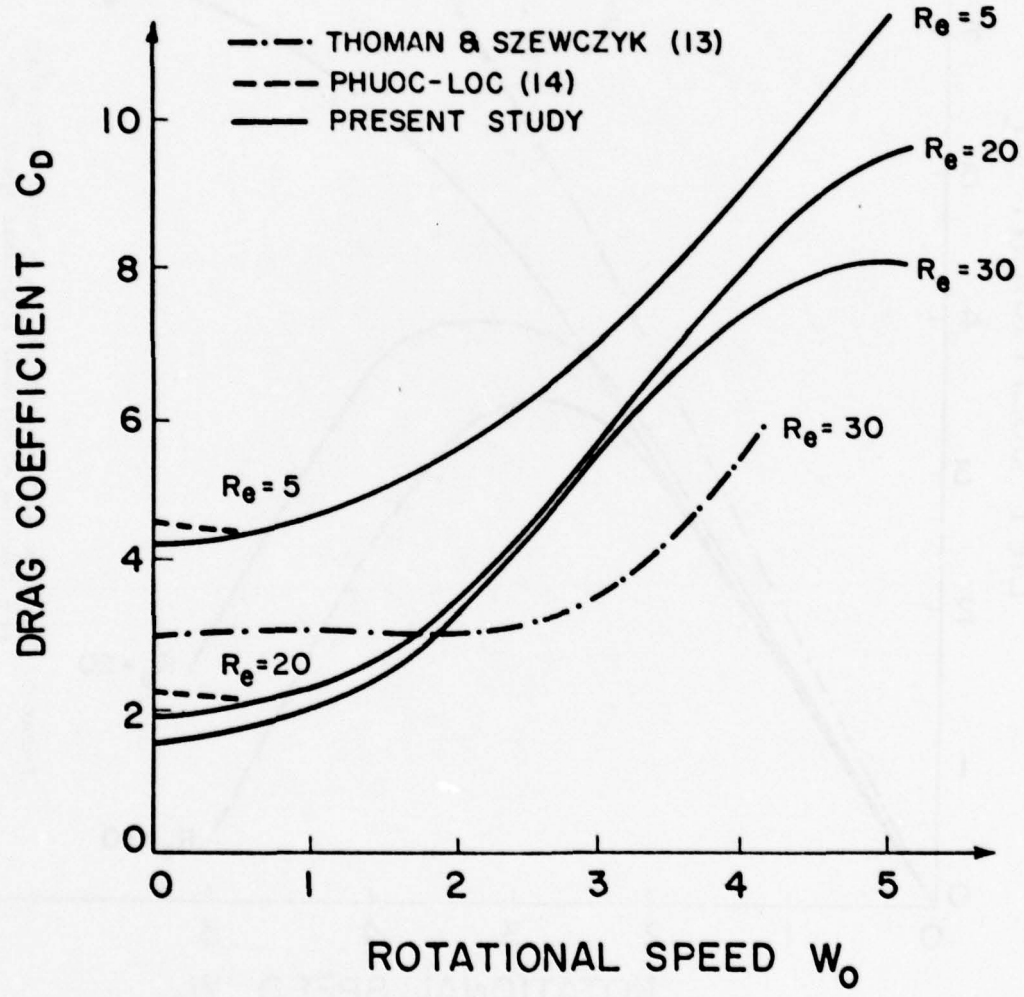

Figure 4. Newtonian drag coefficient, C_D(= total drag/$\rho W^2 a$) as a function of cylinder rotational speed, W_o.

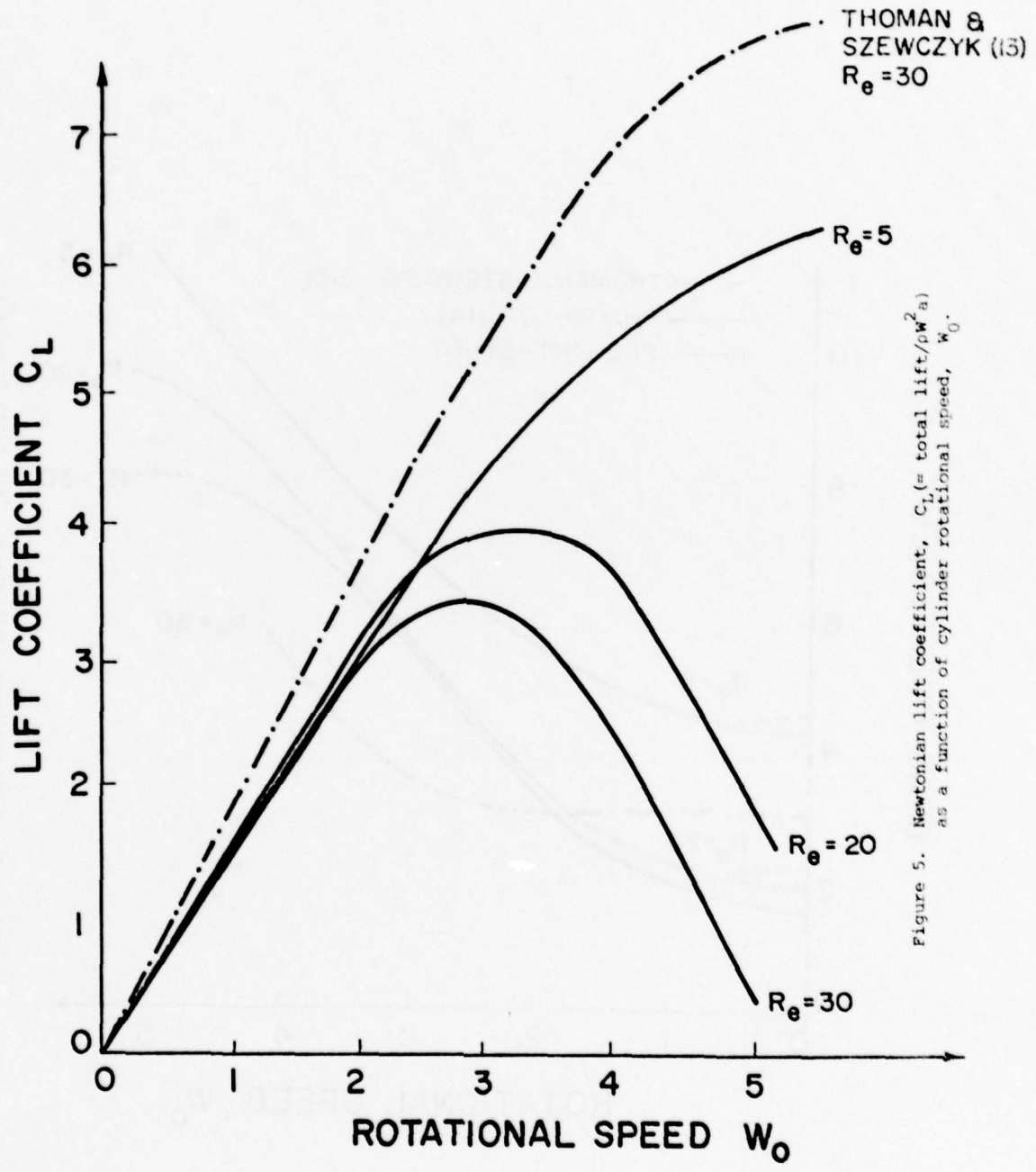

Figure 5. Newtonian lift coefficient, C_L (= total lift/$\rho W^2 a$) as a function of cylinder rotational speed, W_o.

coefficients as functions of the cylinders rotational speed for different Reynolds numbers. It is clear that Phuoc Loc's conclusion [14] that the drag is a slowly decreasing function of rotational speed and that the lift is a linear function of rotational speed, are somewhat premature in view of the very limited range of parameters considered. Far from a decrease, we find a substantial increase in drag as the cylinder is rotated, with some evidence that this increase gradually tails off as the rotational speed increases. This result is qualitatively in agreement with the data of Thoman and Szewczyk [13] but some considerable difference is apparent in actual drag coefficient values.

From Figure 5 it can be seen that the present work predicts a lift force which rises initially to a peak as the rotational speed is increased, but then falls rapidly. The higher the Reynolds number of the mainstream the sooner the lift experienced by the cylinders reaches a maximum and falls away. Again qualitatively we see similar behaviour in the data of Thoman and Szewczyk [13] although they predict very much greater values of the lift coefficient. The results of Phuoc Loc (not shown) essentially lie along the solid lines for Re = 5 and 20, but for such a limited range of $W_0 (W_0 \leq 0.5)$ that they offer no help in resolving the discrepancy between the other two data sets.

In view of the considerable change in lift as the rotational speed is increased, it is of interest to plot the streamline projections for a number of situations. Figures (6-9) show streamline projections for a Reynolds number of 30 and various rotational speeds. It can be seen that the pair of vortices formed behind the cylinder in the stationary case are soon swept away by the rotation of the cylinder and the streamlines near the cylinder are drawn closely around it until one sees a ring of trapped fluid rotating with the cylinder. These results are in excellent agreement with the flow visualization studies of Prandtl and Tietjens [12].

(iii) Visco-elastic flow past a stationary cylinder

From the many investigations available in the literature, both experimental and theoretical, two facts emerge. First, it seems generally agreed that the presence of

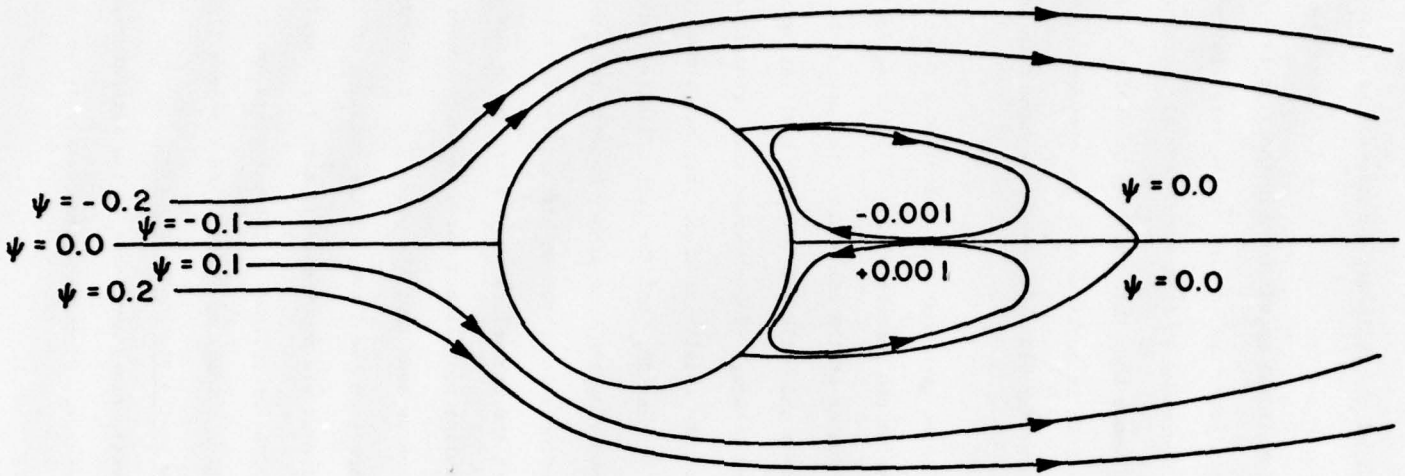

Figure 6. Newtonian streamlines for Re = 30, W_0 = 0.

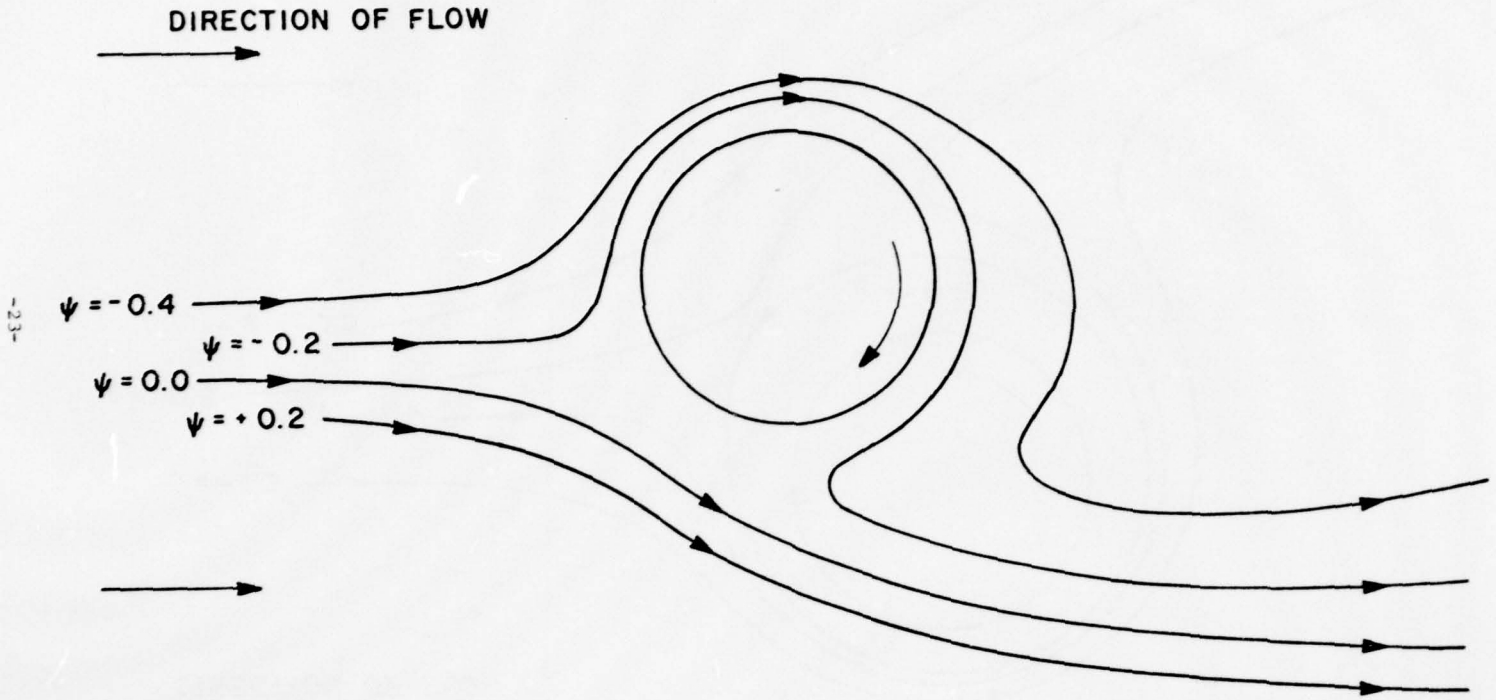

Figure 7. Newtonian streamlines for Re = 30, W_0 = 1.

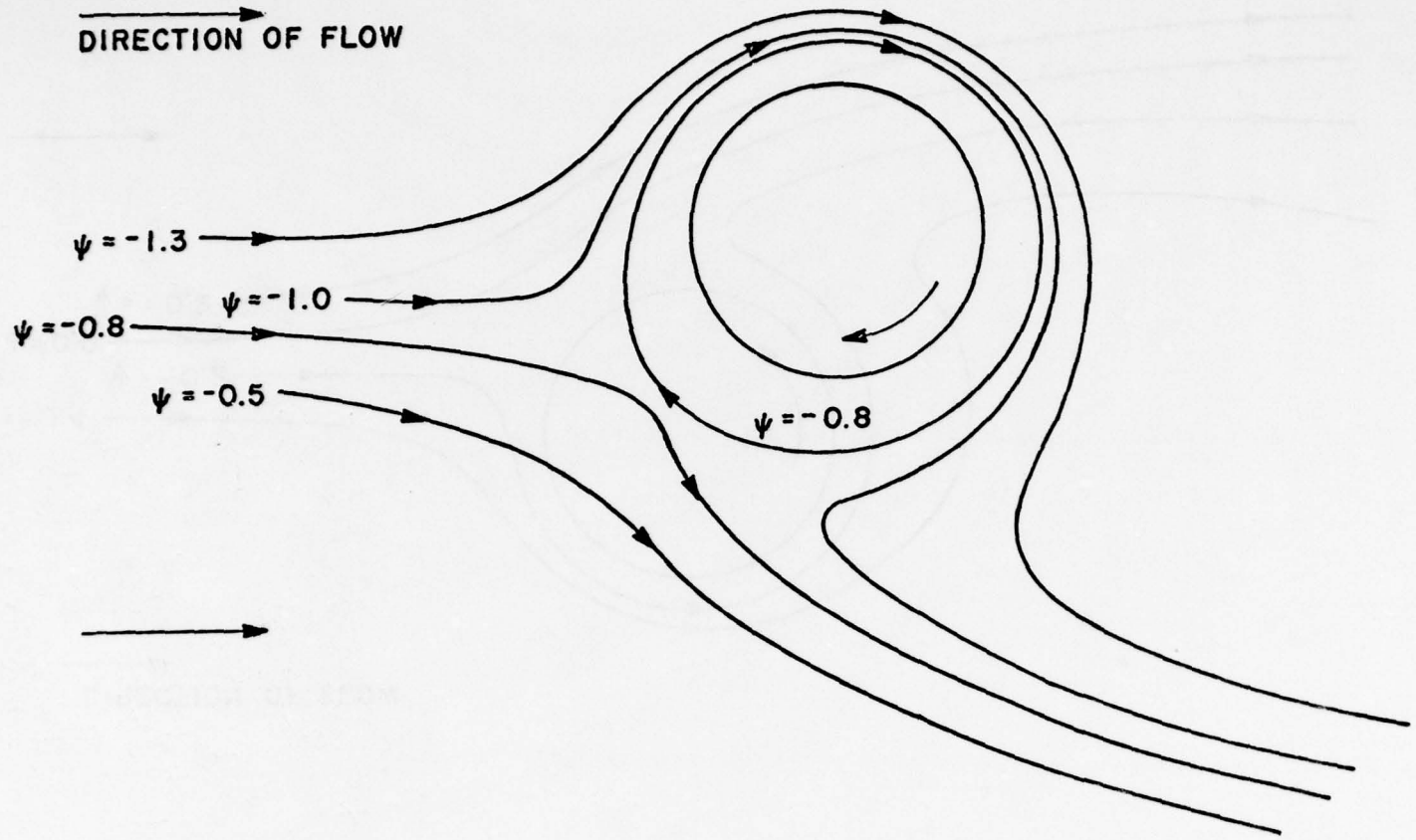

Figure 8. Newtonian streamlines for Re = 30, W_0 = 3.

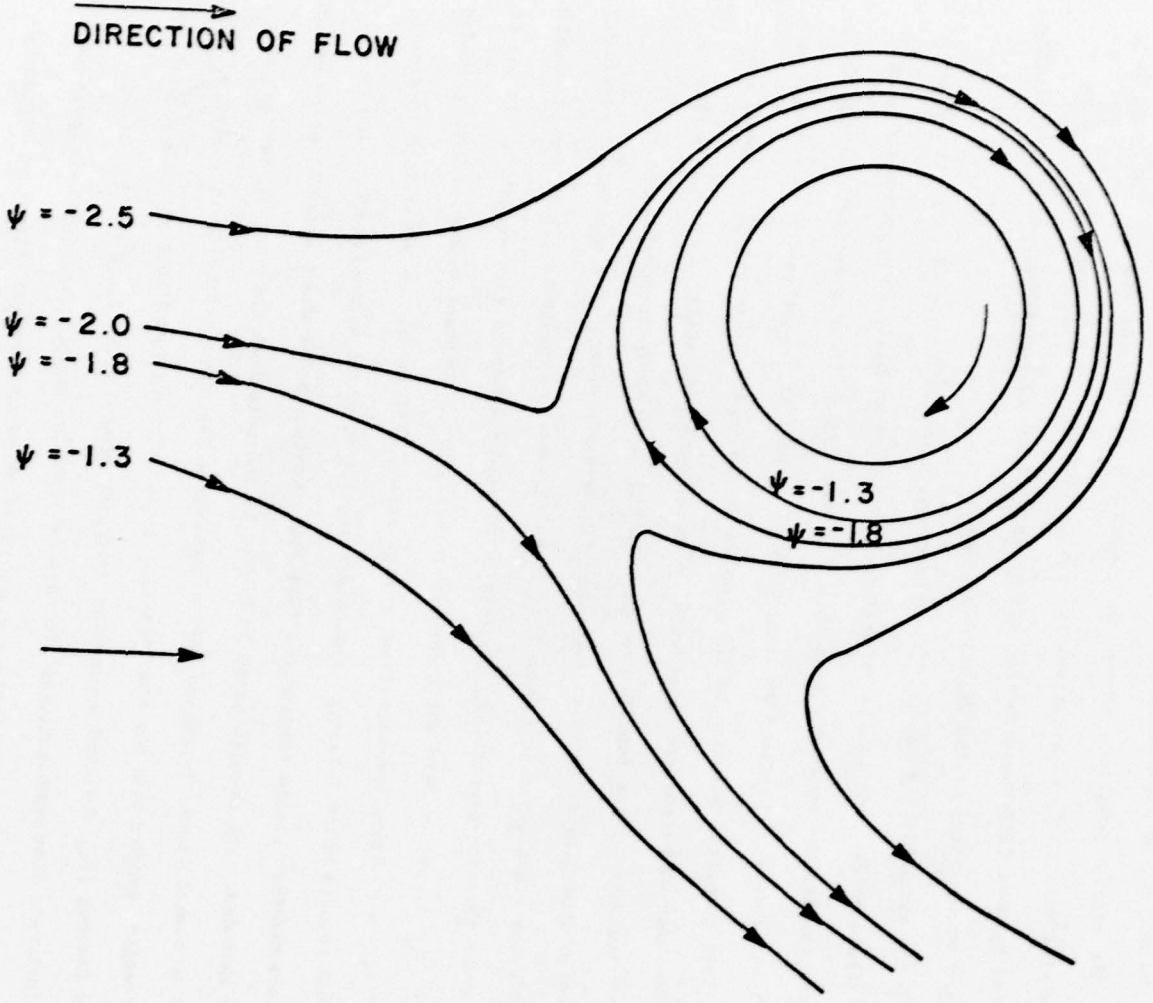

Figure 9. Newtonian streamlines for Re = 30, W_0 = 5.

elasticity induces an initial small decrease in drag at low Reynolds numbers, which charges to a somewhat larger increase in drag as the Reynolds number is increased. Secondly, there is complete disagreement as to whether elastic behaviour in the liquid shifts the streamline pattern upstream or downstream relative to the Newtonian streamlines. The various positions adopted by the many investigations are set out in Table 1. Some related work on flow past a sphere is also included. Recent experimental data presented by Mena [24] suggests that either an upstream or downstream shift are possible depending on the value of the Weissenberg number.

Of the available theoretical investigations, a number have used implicit differential fluid models, but in all cases very restrictive simplifying approximations are employed to make the equations tractible. In some cases, these simplifying assumptions have been severely criticised in later work. The present investigation represents the first full numerical solution of the problem for an implicit visco-elastic model and for the range of parameters considered, a small downstream shift in the streamline pattern was found. The results are shown in Figure 10 where in addition to the Newtonian streamlines, those of two other fluids are plotted. The equivalent vorticity distributions are given in Figure 11. In an attempt to isolate the influence of elastic and shear thinning properties, two sets of Oldroyd parameters were selected. In one of these μ_0 is set to zero which results in a liquid of constant viscosity but, provided $\lambda_1 > \lambda_2$, a positive non-zero first normal stress difference. We shall make reference in the results to an 'elastic' liquid meaning the constant viscosity case, and to a 'visco-elastic' liquid meaning the full four constant model where shear thinning effects are included. The results given in Figure 10 indicate that the small downstream shift due to elasticity is increased when a shear-rate dependent viscosity is included. The streamline projections for the 'elastic' liquid compare favourably with those of Pilate and Crochet [21] who used a constant viscosity second order fluid model. It is unfortunate that computational limitations with the solution technique employed here do not allow us to investigate a wider range of parameters and attempt to reproduce

TABLE 1: RESULTS FROM VARIOUS AUTHORS FOR VISCO-ELASTIC FLOW PAST A STATIONARY CYLINDER (†) OR SPHERE (*)

Investigators	Exptl/ Theory	Streamlines	Drag	Re
Leslie [15]*	T	Downstream	Decrease	<< 1
Ultman and Denn [16]†*	T	Upstream	Decrease	<< 1
	E	Downstream	Decrease	<< 1
James and Acosta [17]†	E	—	Increase	> 1
Mena and Caswell [18]†*	T	Downstream	Decrease	<< 1
Broadbent and Mena [19]†*	E	No Change	Decrease	<< 1
Zana, Tiefenbruck, and Leal [20]*	E	Upstream	—	<< 1
Pilate and Crochet [21]†	T	No Change	Decrease	<< 1
		Downstream	Increase	> 1
Sigli and Coutanceau [22]*	E	—	Decrease	<< 1
	T	Upstream	—	0
Adachi, Yoshioka and Sakai [23]*	E	Upstream	Increase	(·1-60)
	T#	No Shift	Decrease	(·1-60)

#Non-Newtonian, inelastic liquid.

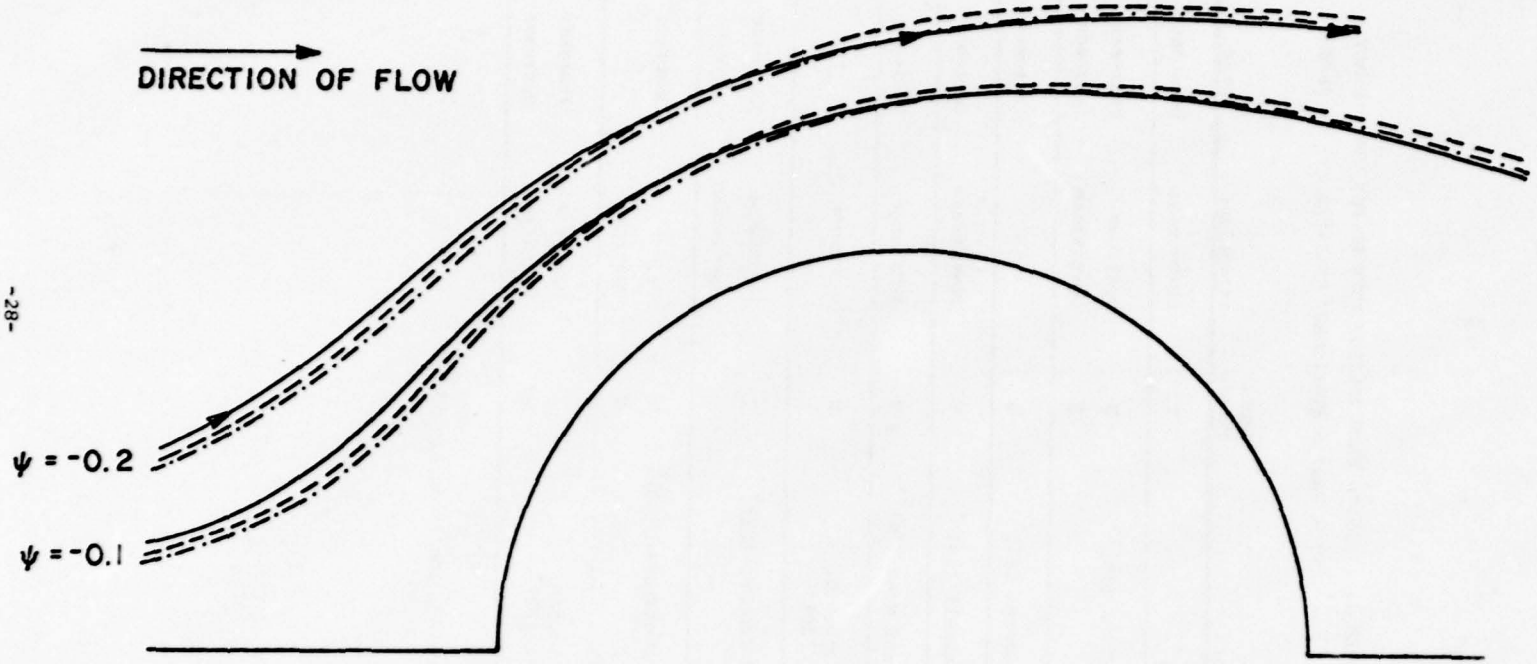

Figure 10. Streamline projections for Re = 10, $W_0 = 0$.
——— Newtonian, – – – Elastic ($\lambda_1^* = 0.6$, $\lambda_2^* = 0.1$, $\mu_0^* = 0.0$)
—·— Visco-elastic ($\lambda_1^* = 0.6$, $\lambda_2^* = 0.1$, $\mu_0^* = 0.1$)

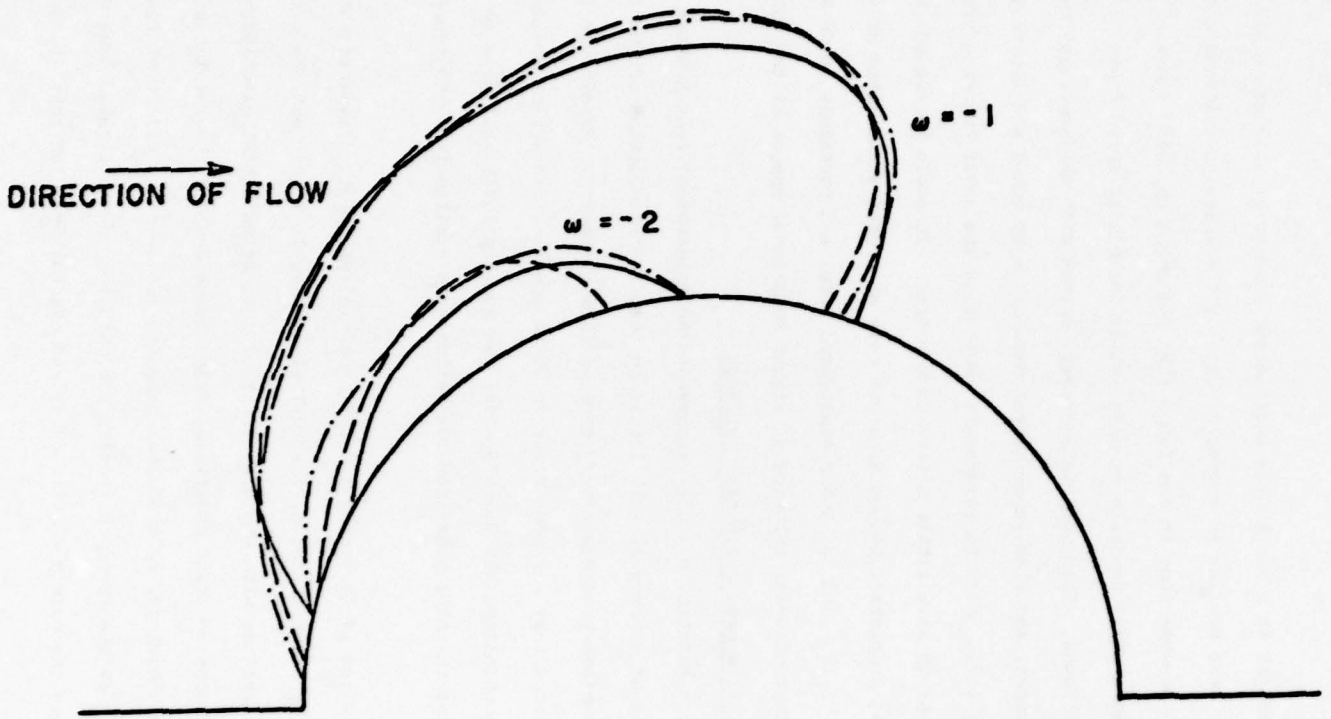

Figure 11. Vorticity distribution for $Re = 10$, $W_0 = 0$
—— Newtonian, – – – Elastic ($\lambda_1^* = 0.6$, $\lambda_2^* = 0.1$, $\mu_0^* = 0.0$)
–·–· Visco-elastic ($\lambda_1^* = 0.6$, $\lambda_2^* = 0.1$, $\mu_0^* = 0.1$)

both upstream and downstream shifting suggested by the latest experimental evidence of Mena [24].

We have chosen not to present drag coefficient results at this stage since they will appear in the next section as a special case of the rotating cylinder data. We remark in passing, however that it was found that for small Reynolds numbers ($Re < 0.1$), elasticity produced a small decrease in drag, while for higher speed flows ($Re > 5$) an increased drag was found. This observation again agrees with the numerical predictions of Pilate and Crochet, and with experimental data given by James and Acosta [17], and Broadbent and Mena [19]. For the parameters considered the shear thinning properties of the liquid appear to have little effect on the drag. It could be argued, however, that shear-thinning properties become apparent only at higher shear rates or with higher values for λ_1, λ_2 and μ_0 than considered here, and certainly we do see later a much greater effect of shear thinning at higher rotational speeds of the cylinder.

(iv) Visco-elastic flow past a rotating cylinder

The flow past a rotating cylinder represents an interesting test problem for a mathematical model of a visco-elastic liquid in that the interaction of the two separate flow mechanisms produces a very complex flow situation. Experience in the past [5] has indicated that for some flows in which one has interacting steady and oscillatory flow mechanisms, the Oldroyd model was qualitatively well able to predict effects due to shear-thinning behaviour but failed even qualitatively to represent elastic effects.

Figures 12, 13 and 14 show drag and lift coefficients plotted against rotational speed for the purely elastic liquid, the full visco-elastic liquid and the equivalent Newtonian liquid. Dealing with the drag first, it can be seen that elasticity appears to contribute an almost constant additional drag independent of the rotational speed. The shear-thinning behaviour, on the other hand has little or no effect at low rotational speeds, but, as the speed increases, the thinning of the liquid seems to reduce the total drag below the purely elastic case, and eventually below that of the Newtonian liquid.

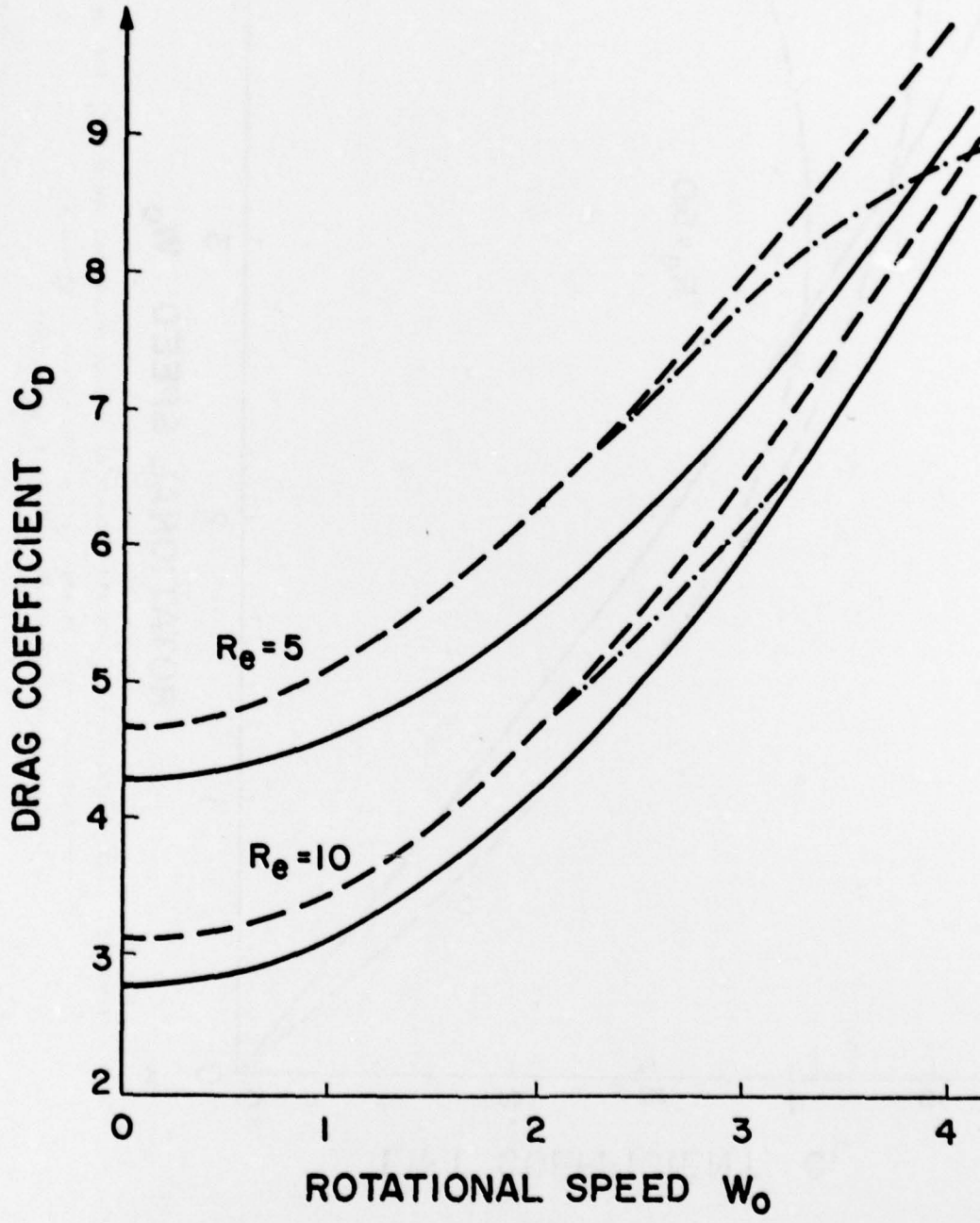

Figure 12. Drag coefficient C_D (= total drag/$\rho W^2 a$) versus rotational speed, W_0
—— Newtonian, --- Elastic ($\lambda_1^* = 0.6$, $\lambda_2^* = 0.1$, $\mu_0^* = 0.0$)
-·-· Visco-elastic ($\lambda_1^* = 0.6$, $\lambda_2^* = 0.1$, $\mu_0^* = 0.01$)

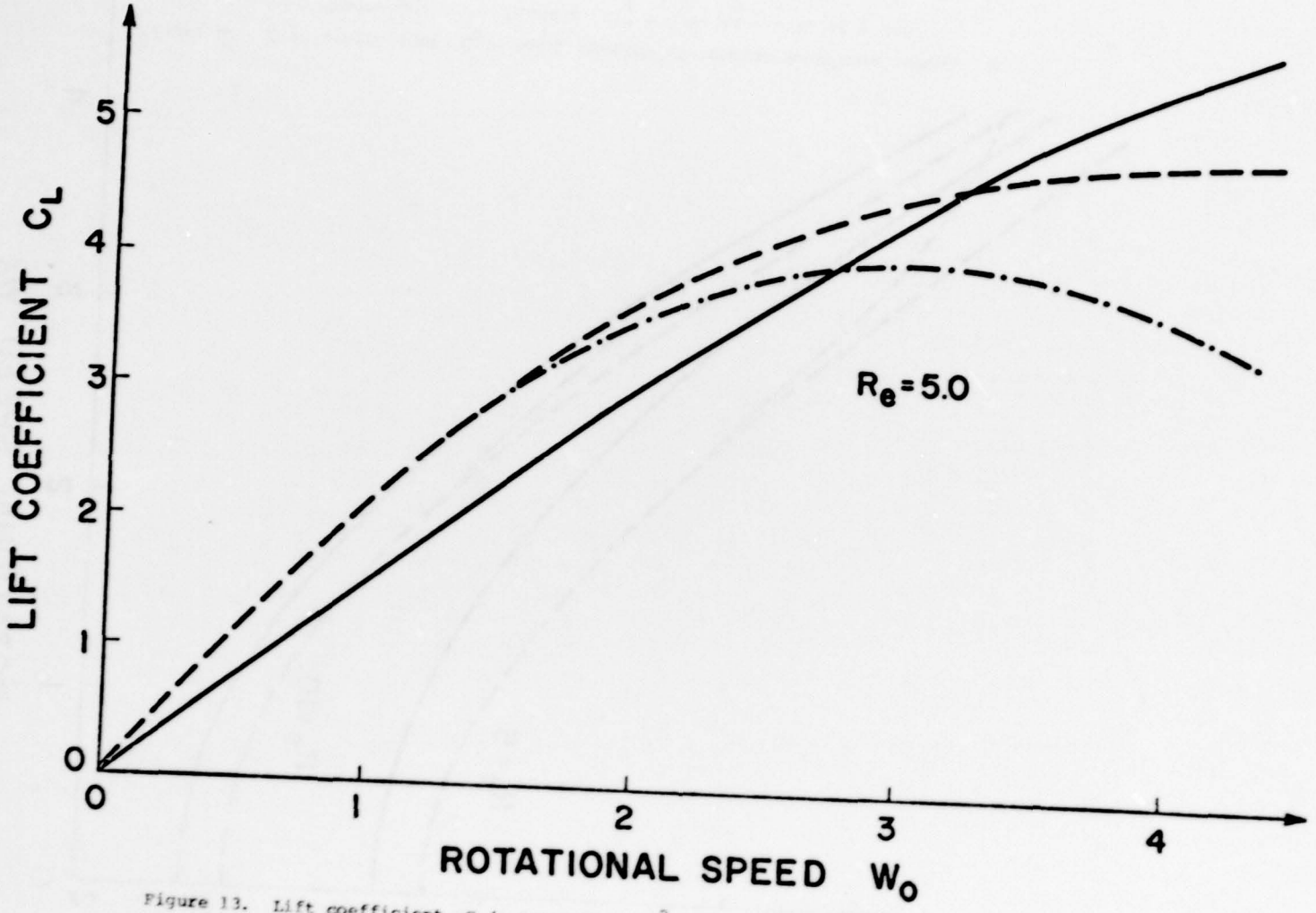

Figure 13. Lift coefficient C_L (= total lift/$\rho W^2 a$) versus rotational speed, W_0 for Re = 5.
—— Newtonian, – – – Elastic ($\lambda_1^* = 0.6$, $\lambda_2^* = 0.1$, $\mu_0^* = 0.0$
–·–· Visco-elastic ($\lambda_1^* = 0.6$, $\lambda_2^* = 0.1$, $\mu_0^* = 0.01$)

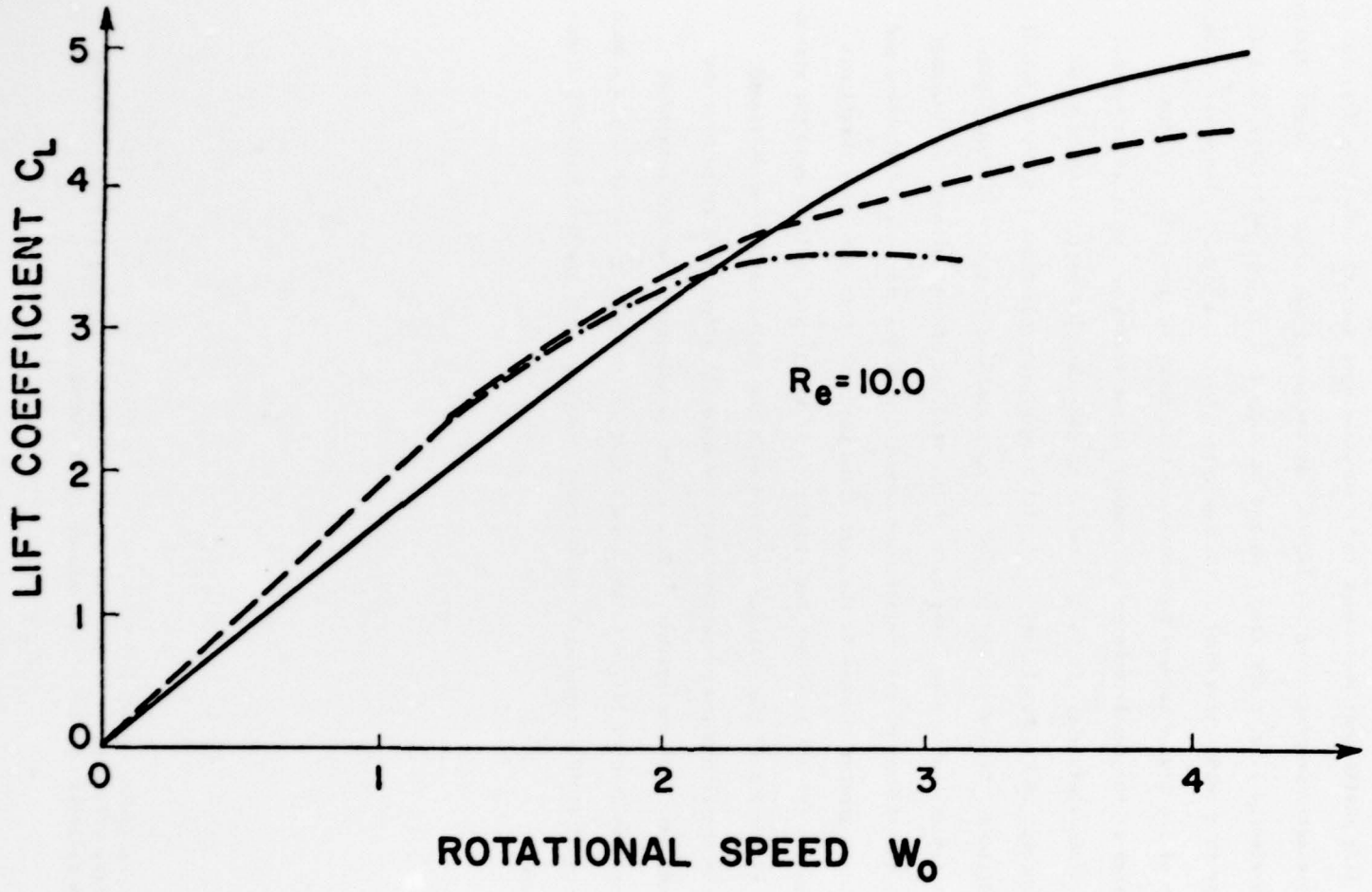

Figure 14. Lift coefficient C_L (= total lift/$\rho W^2 a$) versus rotational speed, W_0 for Re = 10
—— Newtonian, --- Elastic ($\lambda_1^* = 0.6$, $\lambda_2^* = 0.1$, $\mu_0^* = 0.0$)
—·— Visco-elastic ($\lambda_1^* = 0.6$, $\lambda_1^* = 0.1$, $\mu_0^* = 0.01$)

The lift coefficient would seem to be somewhat more sensitive than the drag to the visco-elastic properties of the liquid. At low rotational speeds, for both elastic and visco-elastic liquids one sees a marked increase in lift, but eventually the lift drops away to a value below that of the equivalent Newtonian liquid. The shear-thinning behaviour of the liquid appears to accelerate this decay in the lift coefficient.

In view of the fairly substantial changes in the forces on the cylinder brought about by visco-elasticity, it is of interest to see what flow patterns bring about these changes. In Figures 15 and 16 we plot streamline projections for two different flow conditions. Figures 17 and 18 give the corresponding vorticity distributions. The first remark that one can make is that the rotation of the cylinder considerably amplifies the effects of visco-elasticity compared with the stationary situation, and one sees much greater changes in the streamline patterns. For the lower rotational speed (Figure 15) one sees that the elasticity of the liquid tends to draw the streamlines in closer around the cylinder compared with the equivalent Newtonian liquid, whereas the shear thinning properties have the opposite effect tending to move the streamlines away from the cylinder.# This effect is exaggerated as the rotational speed increases (Figure 16), with the result that for the purely elastic liquid a much larger ring of fluid rotates with the cylinder compared with the Newtonian and visco-elastic cases.

#This latter effect is to be expected in view of the locally higher Reynolds number near the cylinder because of the reduced fluid viscosity.

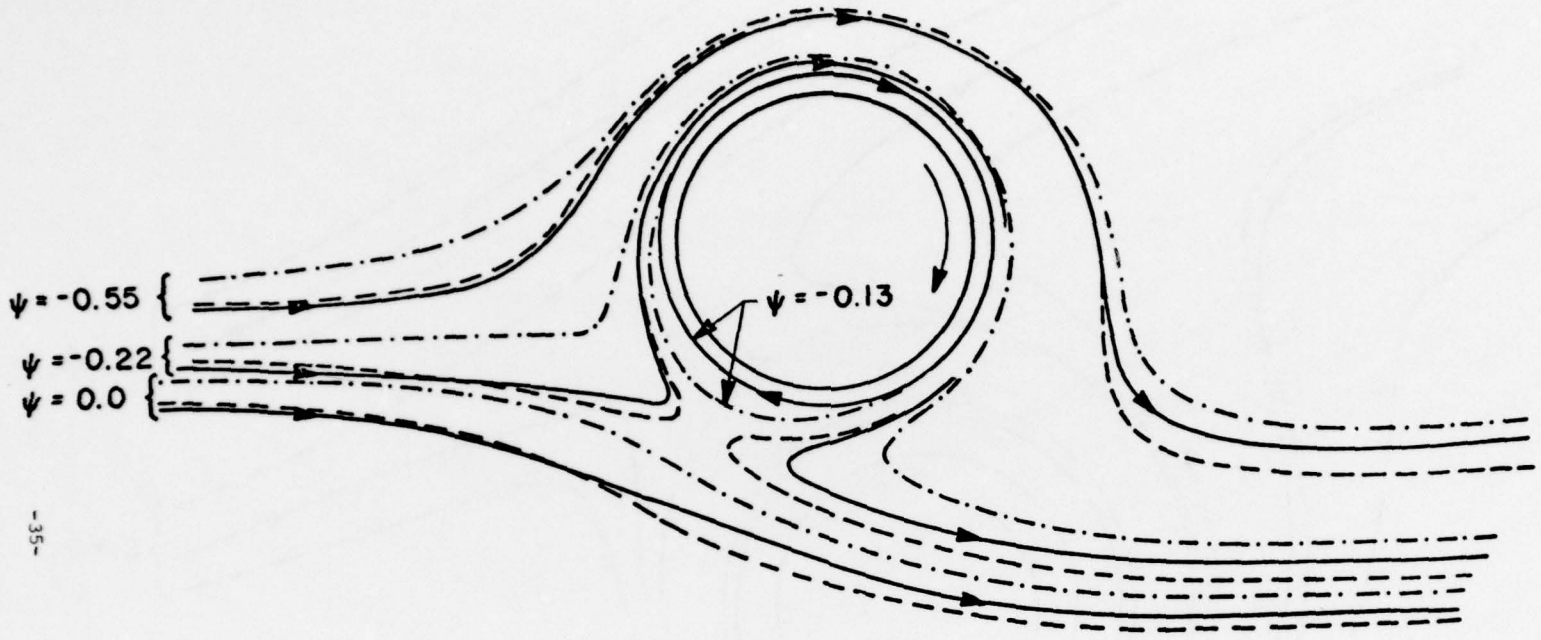

Figure 15. Streamline projections for Re = 5, $W_0 = 1$

—— Newtonian, – – – Elastic ($\lambda_1^* = 0.6$, $\lambda_2^* = 0.1$, $\mu_0^* = 0.0$)

–.–. Visco-elastic ($\lambda_1^* = 0.6$, $\lambda_2^* = 0.1$, $\mu_0^* = 0.1$)

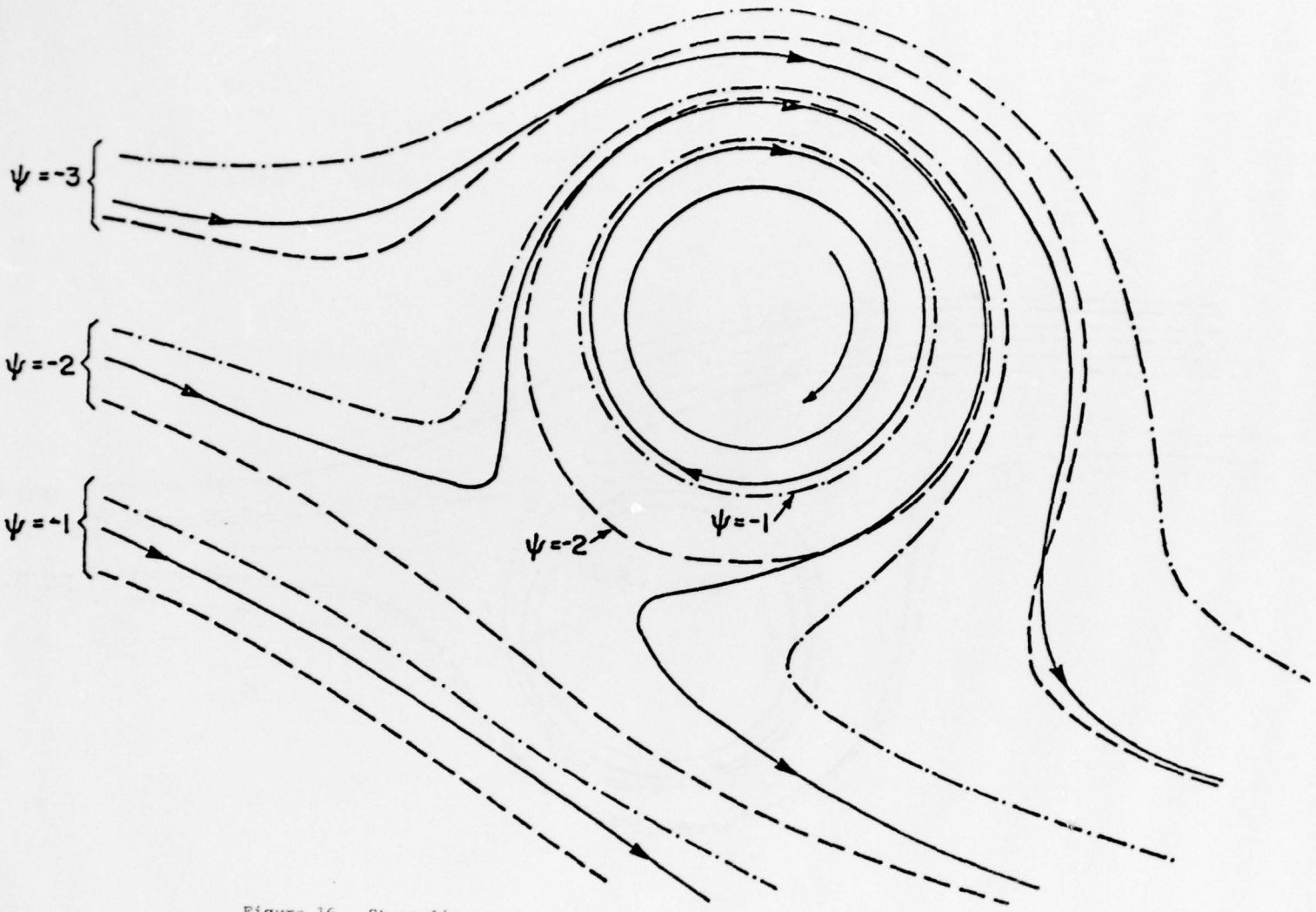

Figure 16. Streamline projections for $Re = 5$, $W_0 = 4$

—— Newtonian, – – – Elastic ($\lambda_1^* = 0.6$, $\lambda_2^* = 0.1$, $\mu_0^* = 0.0$)

–·– Visco-elastic ($\lambda_1^* = 0.6$, $\lambda_2^* = 0.1$, $\mu_0^* = 0.01$)

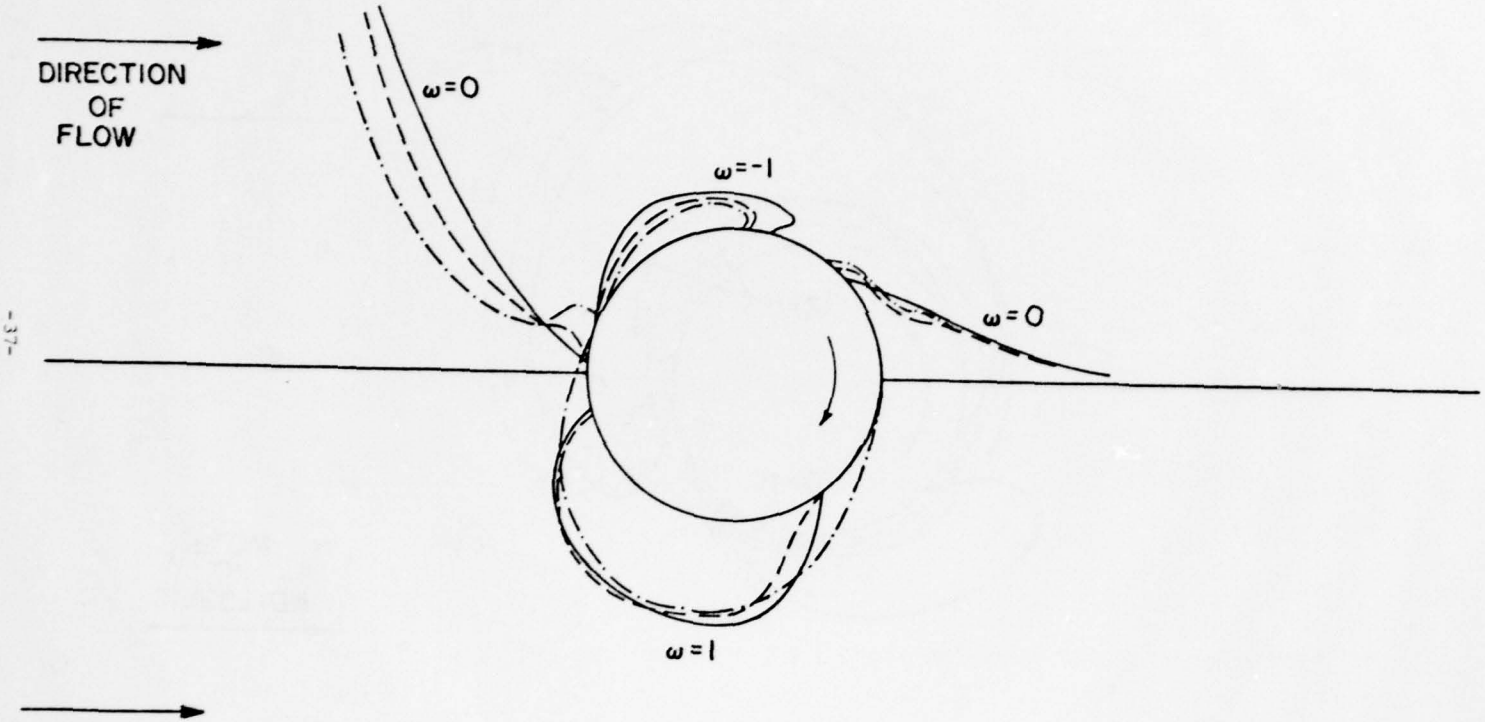

Figure 17. Vorticity distribution for Re = 5, W_0 = 1
—— Newtonian, – – – Elastic (λ_1^* = 0.6, λ_2^* = 0.1, μ_0^* = 0.0)
–·–· Visco-elastic (λ_1^* = 0.6, λ_2^* = 0.1, μ_0^* = 0.1)

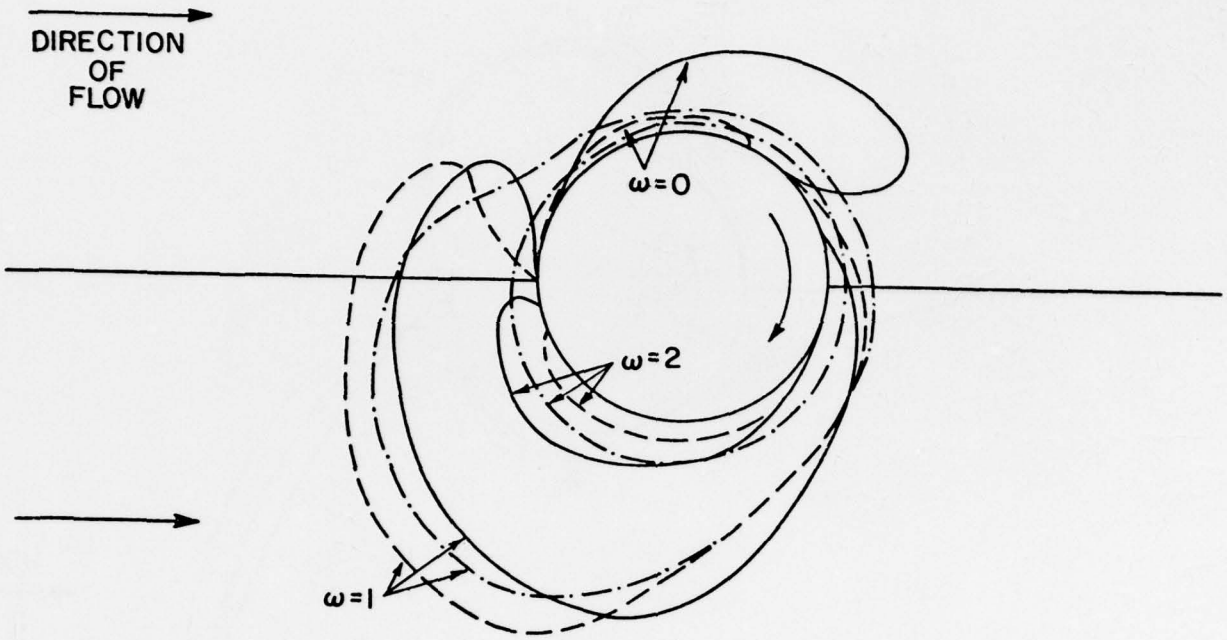

Figure 18. Vorticity distribution for Re = 5, $W_0 = 4$

—— Newtonian, --- Elastic ($\lambda_1^* = 0.6$, $\lambda_2^* = 0.1$, $\mu_0^* = 0.0$)

—·— Visco-elastic ($\lambda_1^* = 0.6$, $\lambda_2^* = 0.1$, $\mu_0^* = 0.01$)

CONCLUSIONS

In this paper we have derived a full numerical solution for the flow of a four constant Oldroyd liquid past a rotating cylinder.

Comparison of the results for a Newtonian liquid and a fixed cylinder, with those of several authors in the literature suggests that the accuracy of the method employed here, in spite of the use of a somewhat coarse finite difference grid, is adequate for our purposes.

For the Newtonian flow past a rotating cylinder, the rotation of the cylinder has a significant effect on the flow, even at low rotational speeds, tending to draw in the streamlines in a 'wrap-around' fashion around the cylinder. So much so that at higher rotational speeds one sees a body of liquid trapped in a constant circulation around the cylinder. The drag and lift coefficients rise rapidly with increasing rotational speed to a peak value, and, in the case of the lift coefficient one sees an equally rapid decay as the rotational speed increases still further.

The effect of elasticity on the streamline pattern for a stationary cylinder is to produce a very small shift downstream. This shift is increased by the presence of shear-thinning properties. A small decrease in drag is found for both elastic and visco-elastic liquids at low Reynolds numbers, becoming a somewhat larger increase in drag at higher Reynolds numbers.

When the cylinder is rotated, the elastic and shear-thinning properties would appear to have opposite effects, the former tending to draw the streamline pattern in even closer around the cylinder compared with the Newtonian case, while the shear-thinning properties seem to have the reverse effect. At low rotational speeds and Reynolds numbers in excess of 5 an increased drag and lift result from the visco-elastic properties of the liquid, but for the shear thinning liquid one sees an eventual decay in drag at higher rotational speeds to below the Newtonian value. For the lift coefficient, for both elastic and visco-elastic liquids, the early increased lift decays at higher rotational speeds to a value below the Newtonian lift, the decay being somewhat more rapid for the visco-elastic liquid.

The very expensive nature of the solution techniques used in this investigation suggests that for highly nonlinear problems there is a need for faster, more sophisticated numerical algorithms to solve the coupled momentum and constitutive equations.

ACKNOWLEDGEMENTS

The author would like to offer sincere thanks to Professor R. B. Bird who first suggested this problem to the author and whose helpful advice and comments have proved invaluable. The author gratefully acknowledges financial support from the Mathematics Research Center, the William F. Vilas Prize Medal Fund (through a grant to Professor Bird), and E. I. Du Pont de Nemours and Company (through a grant to the Rheology Research Center).

REFERENCES

[1] P. Townsend, Rheol. Acta., 12 (1973) 13.

[2] M. G. N. Perera and K. Walters, J. Non-Newtonian Fluid Mech., 2 (1977) 49.

[3] M. G. N. Perera and K. Walters, J. Non-Newtonian Fluid Mech., 2 (1977) 191.

[4] A. R. Davies, K. Walters, and M. F. Webster, J. Non-Newtonian Fluid Mech., 4 (1979) 325.

[5] H. A. Barnes, P. Townsend, and K. Walters, Rheol. Acta., 10 (1971) 517.

[6] C. J. Apelt, A. R. C. Tech. Rep., R & M No. 3175 (1961).

[7] M. Kawaguti and P. C. Jain, J. Phys. Soc. Japan, 21 (1966) 2055

[8] J. S. Son and T. J. Hanratty, J. Fluid Mech., 35 (1969) 369.

[9] S. C. R. Dennis and G. Z. Chang, J. Fluid Mech., 42 (1970) 471.

[10] D. C. Thoman and A. A. Szewczyk, Phys. Fluids, Suppl. II, 2 (1969) 76.

[11] H. Takami and H. B. Keller, Phys. Fluids, Suppl. II, 2 (1969) 51.

[12] L. Prandtl and O. Tietjens, Applied Hydro and Aerodynamics, McGraw Hill, 1934.

[13] D. C. Thoman and A. A. Szewczyk, Tech. Rep. No. 66-14, Heat Transfer and Fluid Mechanics Lab., Un. Notre Dame, 1966.

[14] Ta Phuoc Loc. J. Mec., 14 (1975) 109.

[15] F. M. Leslie, Q. J. Mech. Appl. Math., 14 (1961) 96.

[16] J. S. Ultman and M. M. Denn, Chem. Eng. J. 2 (1971) 81.

[17] D. F. James and A. J. Acosta, J. Fluid Mech. 42 (1970) 269.

[18] B. Mena and B. Caswell, Chem. Eng. J., 8 (1974) 125.

[19] J. M. Broadbent and B. Mena, Chem. Eng. J., 8 (1974) 11.

[20] E. Zana, G. Tiefenbruck and L. G. Leal, Rheol. Acta., 14 (1975) 891.

[21] G. Pilate and M. J. Crochet, J. Non-Newtonian Fluid Mech., 2 (1977) 323.

[22] D. Sigli and M. Contanceau, J. Non-Newtonian Fluid Mech., 2 (1977) 1.

[23] K. Adachi, N. Yoshioka and K. Sakai, J. Non-Newtonian Fluid Mech., 3 (1977/78) 107.

[24] B. Mena, Joint Meeting of the American and Japanese Rheological Societies, Hawaii, 1979.

[25] R. B. Bird, R. C. Armstrong and O. Hassager, *Dynamics of Polymeric Liquids*, Volume 1: Fluid Mechanics, New York, (1977).

[26] J. G. Oldroyd, Proc. Roy. Soc. Lond., A200 (1950) 523.

[27] S. C. R. Dennis and G. Z. Chang, Phys. Fluids 12 (1969) 88.

[28] A. Co, Ph.D. thesis, University of Wisconsin-Madison, 1979.

PT/ed

SECURITY CLASSIFICATION OF THIS PAGE (When Data Entered)

REPORT DOCUMENTATION PAGE

READ INSTRUCTIONS BEFORE COMPLETING FORM

1. REPORT NUMBER: 1980

2. GOVT ACCESSION NO.: (9)

3. RECIPIENT'S CATALOG NUMBER: Technical

4. TITLE (and Subtitle): (6) A NUMERICAL SIMULATION OF NEWTONIAN AND VISCO-ELASTIC FLOW PAST STATIONARY AND ROTATING CYLINDERS.

5. TYPE OF REPORT & PERIOD COVERED: Summary Report, no specific reporting period

6. PERFORMING ORG. REPORT NUMBER:

7. AUTHOR(s): (10) Peter Townsend

8. CONTRACT OR GRANT NUMBER(s): (15) DAAG29-75-C-0024

9. PERFORMING ORGANIZATION NAME AND ADDRESS:
Mathematics Research Center, University of Wisconsin
610 Walnut Street
Madison, Wisconsin 53706

10. PROGRAM ELEMENT, PROJECT, TASK AREA & WORK UNIT NUMBERS: Work Unit Number 3 - Applications of Mathematics

11. CONTROLLING OFFICE NAME AND ADDRESS:
U. S. Army Research Office
P.O. Box 12211
Research Triangle Park, North Carolina 27709

12. REPORT DATE: (11) July [illegible]79

13. NUMBER OF PAGES: 42

14. MONITORING AGENCY NAME & ADDRESS (if different from Controlling Office): (12) 47

15. SECURITY CLASS. (of this report): UNCLASSIFIED

15a. DECLASSIFICATION/DOWNGRADING SCHEDULE:

16. DISTRIBUTION STATEMENT (of this Report)

Approved for public release; distribution unlimited.

(14) MRC-TSR-1980

17. DISTRIBUTION STATEMENT (of the abstract entered in Block 20, if different from Report)

18. SUPPLEMENTARY NOTES

19. KEY WORDS (Continue on reverse side if necessary and identify by block number)

Visco-elastic liquids, Rotating cylinder, Numerical methods

221 200

20. ABSTRACT (Continue on reverse side if necessary and identify by block number)

Numerical solutions are presented for the two-dimensional flow past a circular cylinder in an infinite domain. The flow is assumed to be uniform at infinity and the cylinder is allowed to rotate with a constant angular velocity Ω. Ω is chosen to be in the range $(0 - 5W/a)$ where a is the radius of the cylinder and W is the mainstream velocity at infinity. To incorporate visco-elastic properties into the flow an implicit four constant

(continued)

DD FORM 1 JAN 73 1473 EDITION OF 1 NOV 65 IS OBSOLETE

UNCLASSIFIED

SECURITY CLASSIFICATION OF THIS PAGE (When Data Entered)

Oldroyd model is used, and the resulting nonlinear constitutive equations are solved in parallel with the equations of motion as a coupled set of partial differential equations. The method of solution used is a finite difference technique with block over-relaxation. The results are compared with those of other numerical computations as well as with available experimental data. In particular, consideration is given to the influence of cylinder rotation and of visco-elasticity on the drag and lift experienced by the cylinder and on the streamline patterns and vorticity distribution.